FEBRUARY 2026

IN COMPLIANCE™

THE COMPLIANCE INFORMATION RESOURCE FOR ELECTRICAL ENGINEERS

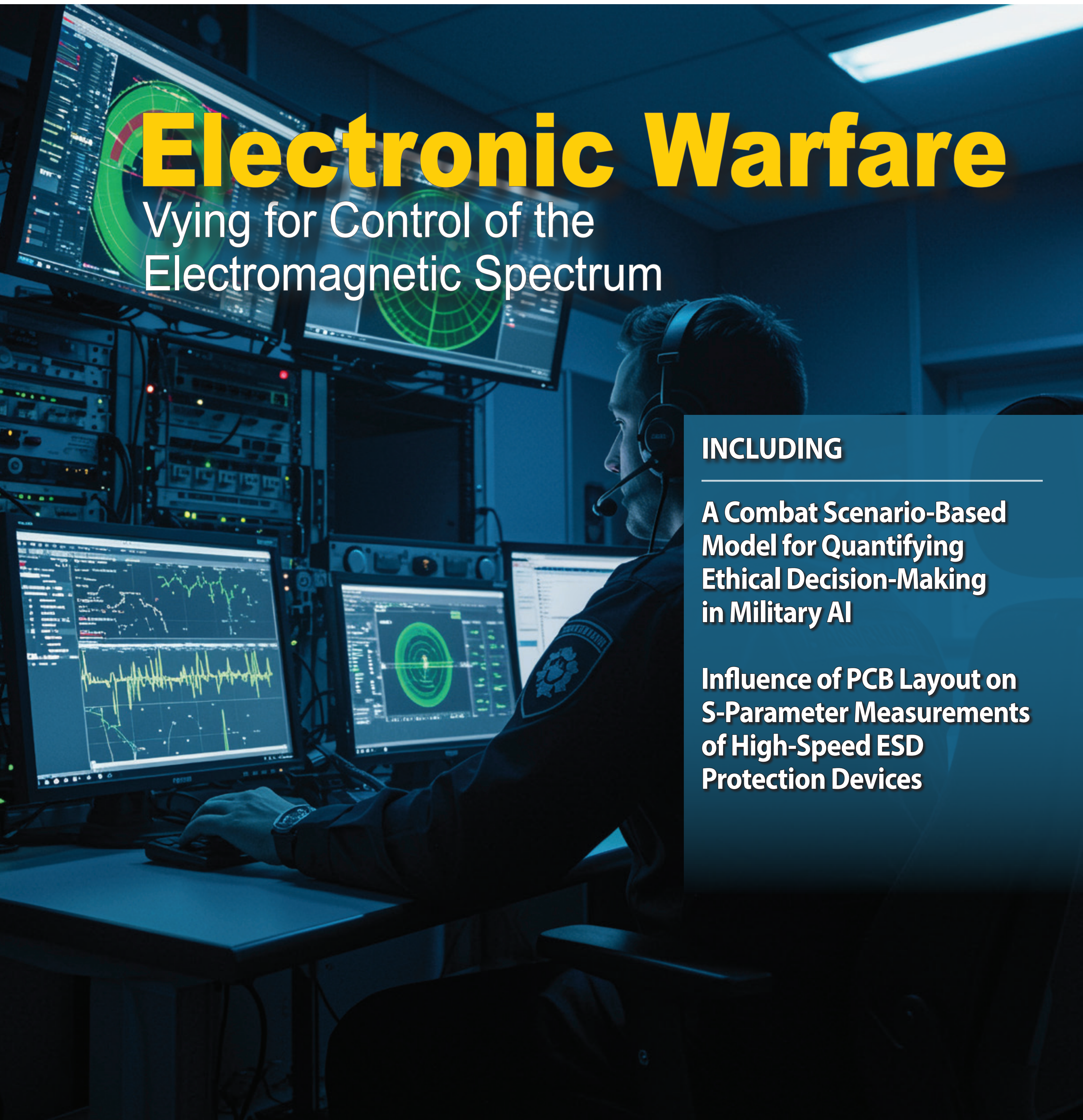

Electronic Warfare

Vying for Control of the Electromagnetic Spectrum

INCLUDING

A Combat Scenario-Based Model for Quantifying Ethical Decision-Making in Military AI

Influence of PCB Layout on S-Parameter Measurements of High-Speed ESD Protection Devices


EXODUS
Best in Class
RF Amplifier SSPA's
POWER
REVEALED
AMP20184
0.8-2.5 GHz, 500W
RF & Microwave
Amplifiers
10KHz-75GHz
AMP20130
80-1000 MHz, 1300W
AMP20192
1.0-2.0 GHz, 10KW
AMP20191
2.0-4.0 GHz, 10KW
AMP20182
4.0-8.0 GHz, 10KW
AMP20178
6.0-18.0 GHz, 400W
AMP20160
1.0-6.0 GHz, 750W
EXODUS ADVANCED
COMMUNICATIONS
3674 E. Sunset Rd, #100
Las Vegas, NV 89120
Tel: 702-534-6564
www.exoduscomm.com

IN COMPLIANCE

In Compliance Magazine
ISSN 1948-8254 (print)
ISSN 1948-8262 (online)
is published by

Same Page Publishing Inc.
451 King Street, #458
Littleton, MA 01460
tel: (978) 486-4684
fax: (978) 486-4691

FEBRUARY 2026

Volume 18 | Number 2

FEATURE ARTICLES

COLUMNS

DEPARTMENTS

FCC Releases Annual Robocall Report

The U.S. Federal Communications Commission (FCC) has released its annual report to Congress detailing consumer complaints and enforcement actions in connection with illegal robocalls.

Released at the end of 2025, the report offers insight into trends related to informal consumer complaints regarding robocalls that were received by the Commission over five full calendar years, from 2020-2024.

Over the five-year period covered in this report, the FCC received a total of 906,622 informal consumer complaints under four different provisions of the Telephone Robocall Abuse Criminal Enforcement and Deterrence Act (TRACED Act). The total number of informal complaints during the most recent five-year reporting period represents a significant decrease from the 1,351,317 informal complaints received during calendar years 2019-2023, with most of the decreases occurring in 2023 and 2024.

This year's report confirms that the FCC's stepped-up enforcement efforts over the past several years are continuing to have a positive impact in reducing the number of informal consumer complaints. After a record 333,146 informal complaints filed in 2018, annual informal complaint numbers have generally seen marked declines, with just 135,268 informal complaints filed in 2023, and 159,804 complaints filed in 2024.

Report Says Insufficient FDA Staffing Limits Oversight of Med Device Recalls

Efforts by the U.S. Food and Drug Administration (FDA) to oversee the recall of faulty medical devices are being directly impacted by insufficient staffing at the agency.

This news comes straight from the U.S. Government Accountability Office (GAO). According to a report issued by the agency in early December, the FDA failed to meet its 3-month target for terminating manufacturer-initiated device recalls during the five-year period from fiscal years 2020 through 2024, with nearly 74% of recalls exceeding the 3-month termination goal.

The reason for the FDA's oversight failure? According to the GAO report, "Insufficient staff limit FDA's ability to conduct oversight activities." The potential consequences? Insufficient staffing "can create inefficiencies in the process and potentially put lives at risk."

According to an article posted to the MedTechDive website, the GAO's report of oversight of medical device recalls was initiated by a Congressional request in late 2023. Further, the timeframe detailed in the GAO report occurred before the U.S. Department of Health and Human Services (HHS) initiated significant staff reductions in February and April 2025, which included personnel working to support the inspection of medical devices, drugs, and vaccines.

The GAO report includes several recommendations to address the staffing gap on medical device oversight, including strategic increases in staffing and revising regulations to require device manufacturers to implement FDA recommendations for manufacturer-initiated recalls.

Astronomers Discover a Lemon-Shaped "Exoplanet"

A lemon-shaped planet?? That's what astronomers using the James Webb Space Telescope have recently discovered circling a small, dense star. According to an article posted to the website of Scientific American, the odd-shaped "exoplanet," named PSR J2322-2650b, is roughly the size of the planet Jupiter, featuring an elongated shape resembling a lemon.

The exoplanet circles a small, dense star known as a pulsar. Researchers believe that the star's proximate gravity was the key element that pulled the exoplanet into its current shape. But the exoplanet's shape is not the most intriguing thing about the discovery.

The exoplanet's atmosphere is rich in carbon but contains no nitrogen or oxygen. According to the Scientific American article, when researchers observed the emission spectrum of the exoplanet's atmosphere, they found wavelengths that aligned with molecular carbon. They also speculate that molecular carbon could be at the core of the planet in the form of diamonds!

Why Heel Straps Fail in Real ESD Environments

Most facilities rely on heel straps without understanding how gait, flooring behavior, and contact geometry make system-level flooring and footwear evaluation essential.

Why are heel straps still widely used even though their performance often falls short in real ESD environments?

Heel straps remain the default in most factories. They are inexpensive, easy to deploy, and reliably pass basic resistance checks. In qualification testing, test subjects may not represent how people actually walk, masking inconsistent results that depend heavily on individual gait. Research in gait analysis shows ~ 60–65% of individuals maintain consistent heel-first contact, while 8–12% are habitual forefoot or toe walkers, meaning their heel straps may never touch the floor. ANSI/ESD STM 97.2 lab experiments show floor peak voltages ranging from <30 volts on conductive rubber to >200 volts on conductive vinyl and epoxy, depending on footwear, partially covered by a strap. Without continuous contact as people walk, charge accumulates and cannot discharge until the strap touches the floor.

What grounding system options provide more reliable, full-cycle electrical continuity than heel straps?

Full-coverage sole straps and ESD shoes address the core deficiency of heel straps: minimal, inconsistent contact with the floor. Sole straps extend conductive material across both heel and forefoot, engaging the flooring throughout the entire stance phase rather than at a single point, significantly improving continuity and reducing walking-voltage fluctuations. ESD shoes further enhance reliability by integrating conductive elements into the outsole and midsole, eliminating common human failures such as misaligned straps, worn contact patches, or improper fit.

Footwear and flooring must always be evaluated as a system. Most ESD floors are roughly 95% insulative, with grounding achieved through conductive granules or carbon veins. These surfaces generate static during movement and rely on footwear contact for discharge, making a strong case for low-generating floor materials.

How does selecting the right ESD flooring influence engineering outcomes and ESD-program performance?

Selecting the right ESD flooring has a disproportionate impact on engineering outcomes because the floor is the foundation of all grounding within an EPA, excluding the work surface. The floor establishes the reference plane that personnel, carts, chairs, fixtures, and mobile equipment must couple to. Programs that focus narrowly on personnel grounding while overlooking wheels, casters, seating, and maintenance pathways often create hidden voltage differentials within the EPA.

Flooring selection also directly influences the walking-voltage component of ANSI/ESD S20.20, the parameter most closely tied to real-world ESD failures. High-generating or finish-dependent floors introduce variability, maintenance burden, and long-term instability. Low-generating, maintenance-stable ESD floors like conductive rubber provide consistent charge control, predictable process behavior, and common electrical potential across the entire environment, conditions essential for reliable high-yield manufacturing.

staticWorx®

Engineering flooring-based ESD control systems grounded in research and real-world performance.

Specialists in personnel grounding and walking-voltage mitigation

Contributors to ANSI/ESD standards education

Advocates for system-level ESD program design

David Long
Founder & Technical Director
StaticWorx

"ESD-control flooring products work as a system, not as individual components."

STANDARDS PRACTICE

ESD Testing Parameters

By Karen Burnham

There are lots of different ESD testing standards out there, and most of them have a schematic similar to the one above from MIL-STD-461G. However, if you look across multiple standards, you'll see that Rd and Cd can have different values. I recently had an aerospace client who would normally test to CS118 from the MIL-STD. But, due to a particular threat environment, we recommended applying a harsher test from the automotive world. CS118 has a maximum test at ±15 kV, but we thought a ±25 kV test would be appropriate.

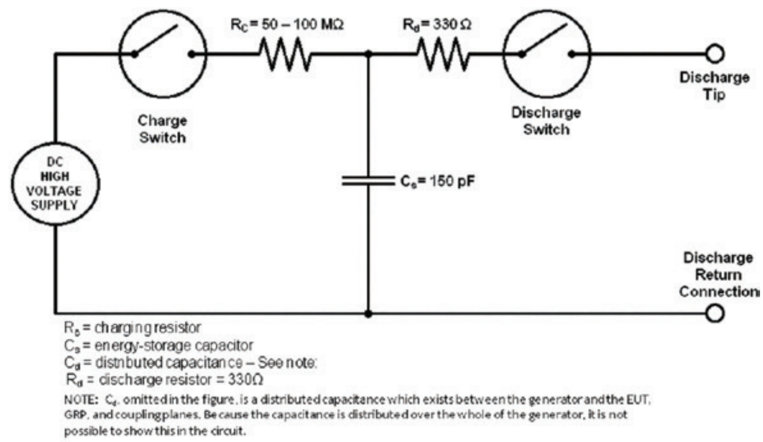

FIGURE CS118-1. Simplified diagram of the ESD generator.

In looking at ISO 10605 to remind myself of the parameters of the ±25 kV discharge, I was reminded that Rd and Cd vary with different tests, and I wanted to make sure that I was using the appropriate value. The ISO standard has two options for both the resistor and capacitor. The cap can be 150 or 330 pF, and the resistor can be 330 or 2000 Ω. Thanks to these values being standard in both ISO and IEC 61000-4-2, they can be found in most off-the-shelf ESD guns. So, which values should you use if you're testing beyond a specific standard?

For the capacitor, if the main threat is from a human interaction, the IEC document recommends 150 pF as the standard. ISO 10605 recommends choosing 330 pF when testing equipment that a human might interact with while in the interior of the vehicle and 150 pF for equipment that may be accessed from the exterior. The larger 330 pF value represents something closer to the capacitance of the human/car system, while the 150 pF value represents a "free floating" (if you'll forgive me) human.

For the resistor, the standards are clear that 330 Ω represents the discharge occurring from a human through a metal tool to the target. Imagine approaching a piece of hardware with a wrench in hand and a spark jumping from the tip of the wrench to the hardware. Because of the lower resistance allowing for more current to flow, this is considered the harsher test and is usually the default. The 2 kΩ resistor is a better representation of a discharge directly from human skin, such as might occur when a user goes to push a button.

For this particular aerospace client, we were most concerned about a human moving independently of the vehicle and interacting with units through touch interfaces, not using tools. So, we chose a ±25 kV discharge with a 150 pF cap and 2 kΩ resistance. I should note that ISO 10605 recommends a maximum discharge of ±15 kV when using a 330 pF cap, so that's another argument for choosing the 150 pF test.

As a side note, one of the other options to consider for ESD testing is whether contact or air discharge is appropriate. Annex B of ANSI C63.16 has useful guidance on that point, discussing when air vs. contact is appropriate. The short version is that while contact discharge is more repeatable, air discharge is more representative of ESD events out in the field.

One other standard to keep in mind when designing a custom ESD test is MIL-STD-1541, now officially discontinued (but freely available). It shows the circuit schematic for an ESD test that can provide a much wider range of discharge types than the tests based on IEC 61000-4-2. You can see a recent document using this in NASA-HDBK-4002B, where they have a MIL-STD-1541 setup tailored to represent discharges on the exterior of spacecraft due to the space charging environment.

PRACTICAL ENGINEERING

Noise Suppression Techniques Using Capacitors

By Don MacArthur

Capacitors play a crucial role in reducing electromagnetic interference (EMI) by acting as filters that block unwanted high-frequency noise while allowing the desired signal to pass through. They achieve this by storing and releasing electrical energy, which helps to smooth out voltage fluctuations and suppress noise. Capacitors are often used in conjunction with inductors to form LC filters, which are effective in attenuating EMI across a wide range of frequencies.

TYPES OF CAPACITORS USED IN NOISE SUPPRESSION

There are several types of capacitors commonly used in noise suppression, each with its own unique characteristics and applications:

1. Ceramic Capacitors: These are widely used due to their small size, low cost, and high reliability. They are suitable for high-frequency applications and are often used in decoupling and bypassing circuits.
2. Film Capacitors: Made from thin plastic films, these capacitors offer good stability and low inductance, making them ideal for high-frequency noise suppression. They are commonly used in audio and RF applications.
3. Electrolytic Capacitors: These capacitors have high capacitance values and are used in applications requiring large energy storage. They are often used in power supply circuits to filter out low-frequency noise.
4. Safety Capacitors (Class-X and Class-Y): These capacitors are designed to protect against electrical shock and are used in AC line filtering to suppress EMI/RFI. Class-X capacitors are connected across the AC line, while Class-Y capacitors are connected between the AC line and ground.

DESIGN CONSIDERATIONS FOR CAPACITORS IN NOISE SUPPRESSION

When selecting and placing capacitors for optimal noise suppression, several design considerations should be considered:

1. Capacitance Value: Choose a capacitance value that matches the frequency of the noise to be suppressed. Higher capacitance values are effective at lower frequencies, while lower capacitance values are suitable for higher frequencies.
2. Self-Resonant Frequency: Ensure that the capacitor's self-resonant frequency is higher than the frequency of the noise to be suppressed. This helps to maintain the capacitor's effectiveness in filtering out unwanted signals.
3. Placement: Place capacitors as close as possible to the noise source or the sensitive circuitry to minimize the length of the conductive path and reduce the impact of parasitic inductance.
4. Type of Capacitor: Select the appropriate type of capacitor based on the application and the frequency range of the noise. For example, ceramic capacitors are ideal for high-frequency noise suppression, while electrolytic capacitors are better suited for low-frequency applications.
5. Temperature Stability: Consider the temperature stability of the capacitor, especially in applications where the operating temperature may vary. Some capacitors, such as ceramic capacitors, can experience changes in capacitance with temperature fluctuations.

SUMMARY

By carefully selecting and placing capacitors, engineers can effectively reduce EMI and ensure the reliable operation of electronic circuits.

MILITARY AND AEROSPACE EMC

High Intensity Radiated Fields *Part 4*

By Patrick André

In previous issues [1-3], we have established the need for HIRF testing and the field strengths that equipment needs to survive. But how are these levels used to test the aircraft? How do they relate to the test levels found in DO-160 and other standards?

The SAE has a series of aerospace recommended practices (ARPs) used for the certification of aircraft and to support FAA Advisory Circulars. Two we will look at are ARP60493, Guide to Civil Aircraft Electromagnetic Compatibility (EMC), and ARP5583A, Guide to Certification of Aircraft in a High-Intensity Radiated Field (HIRF) Environment, which is intended to be "consistent with the certification steps described in AC 20-158." [4]

The decision-making process and the details for Level A HIRF Safety are extensive. The FAA has supplied a flow chart of this process, which can be found in Figure 1. A follow-on chart for Step 10 is provided in Figure 2.

An important aspect of determining an aircraft's ability to handle HIRF is finding its transfer function. The transfer function is the attenuation of the aircraft over frequency. A radiated field test is performed on the aircraft to determine the transfer function. A field of a known level is induced on the aircraft using a variety of methods. These can include direct field radiation by antennas or by using a cage around the aircraft body, wings, and so forth. The fields may be either high or low level.

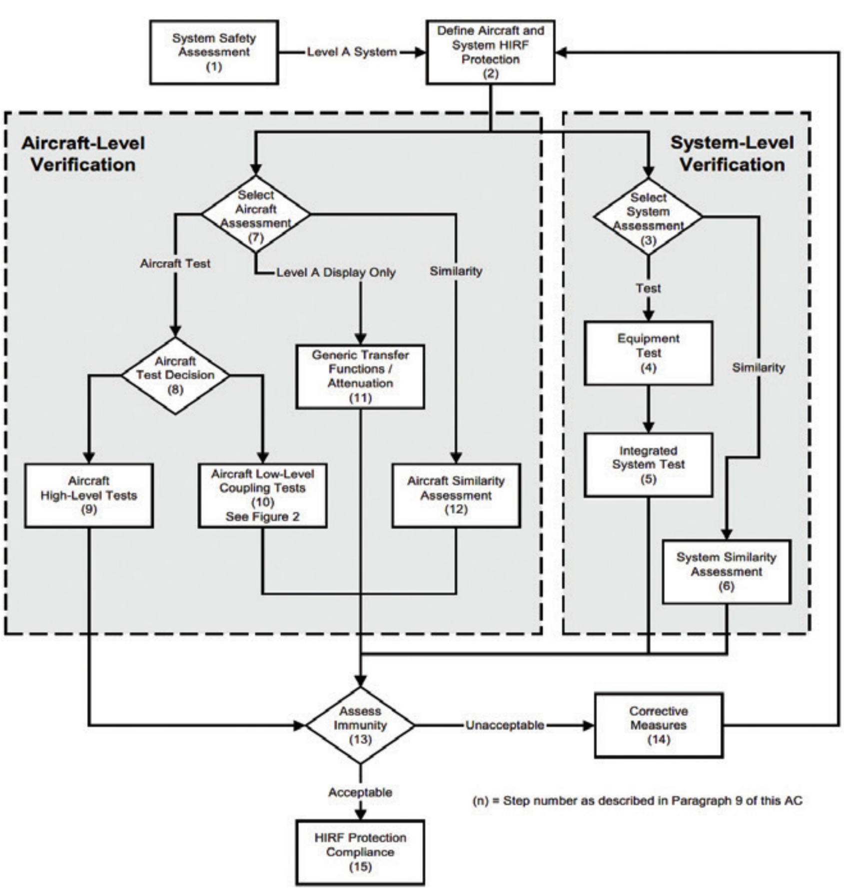

Figure 1: Routes to HIRF Compliance for Level A Systems (From AC 20-158B)

One method used is called Low Level Direct Drive (LLDD). The aircraft body is induced directly, say, at the nose of the aircraft with an RF current. The current will flow over the body of the aircraft and radiate to the cage. The end of the aircraft, which is farthest from the drive point (e.g., the tail or wing tip), is terminated to the cage through a load. This is best performed once a known field produces a known current in the skin of the aircraft. This method is used for testing below 400 MHz, while the Low-Level Swept Field (LLSF) test is best from 100 MHz to 18 GHz. [5]

Using LLDD, the currents induced onto the internal cables can be measured. Recording the currents induced on various cables will be used to determine the attenuation of the aircraft. These levels can be plotted similarly to conducted immunity test plots. Once derived, a limit can be created, which is an envelope over these values. An example is shown in Figure 3, where four measurements are taken, and a limit line is found that encloses all measured data.

However, during development, no airframe is available to obtain these levels. In this case, generic limits are given by AC 20-158B for various aircraft sizes and for rotorcraft. These levels are derived to ensure that 95% of the population of aircraft will be covered. But note that they may be higher than required for a particular airframe. If designs are created to meet these levels, the equipment may be overdesigned, increasing its weight and size as a result, neither of which is desirable on a commercial aircraft.

Please note that these limits are normalized for a 1 V/m test. If an aircraft needs to meet 100 V/m, this limit line must increase by the same amount (100 times, or 40 dB). Be sure to properly scale all induced current levels for the likely field strengths to which the aircraft will be exposed.

This is only one of several steps in the certification process for an aircraft. The criticality of the equipment must be determined to establish if it is Level A, B, or C. For Levels B and C, equipment testing is adequate for certification. Most test levels will be reasonably easy to meet by HIRF standards, likely Category R or less.

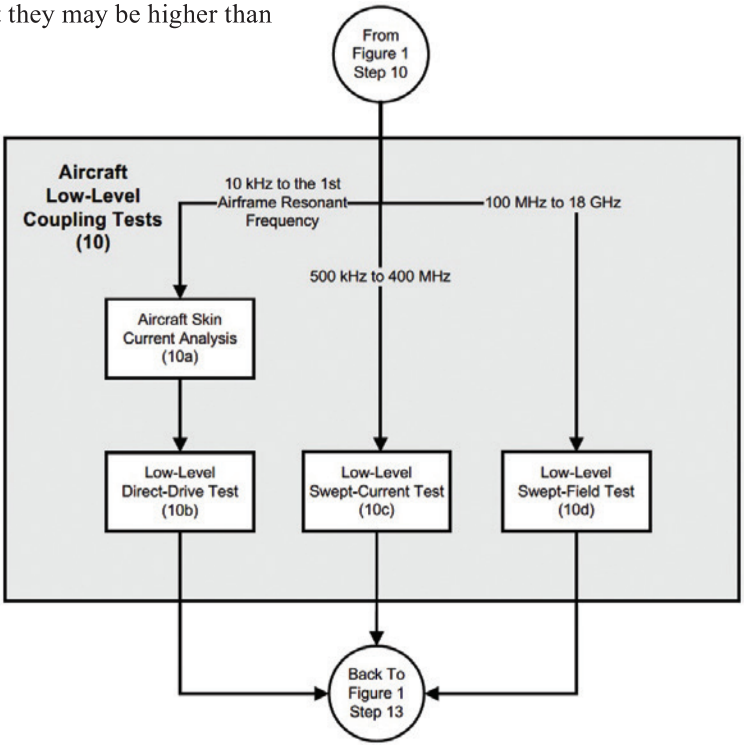

Figure 2: Aircraft Low-Level Coupling Tests for Level A Systems (From AC 20-158B)

ENDNOTES

1. "High Intensity Radiated Fields (HIRF), Part 1", *In Compliance Magazine*, July 2025.
2. "High Intensity Radiated Fields (HIRF), Part 2", *In Compliance Magazine*, September 2025.
3. "High Intensity Radiated Fields (HIRF), Part 3", *In Compliance Magazine*, November 2025.
4. SAE Aerospace, ARP5583A, Guide to Certification of Aircraft in a High-Intensity Radiated Field (HIRF) Environment, (SAE International, 2010), pg. 1.
5. Details of this method can be found in FAA 20-158B, paragraph 10, and are further defined in ARP5583 and elsewhere.

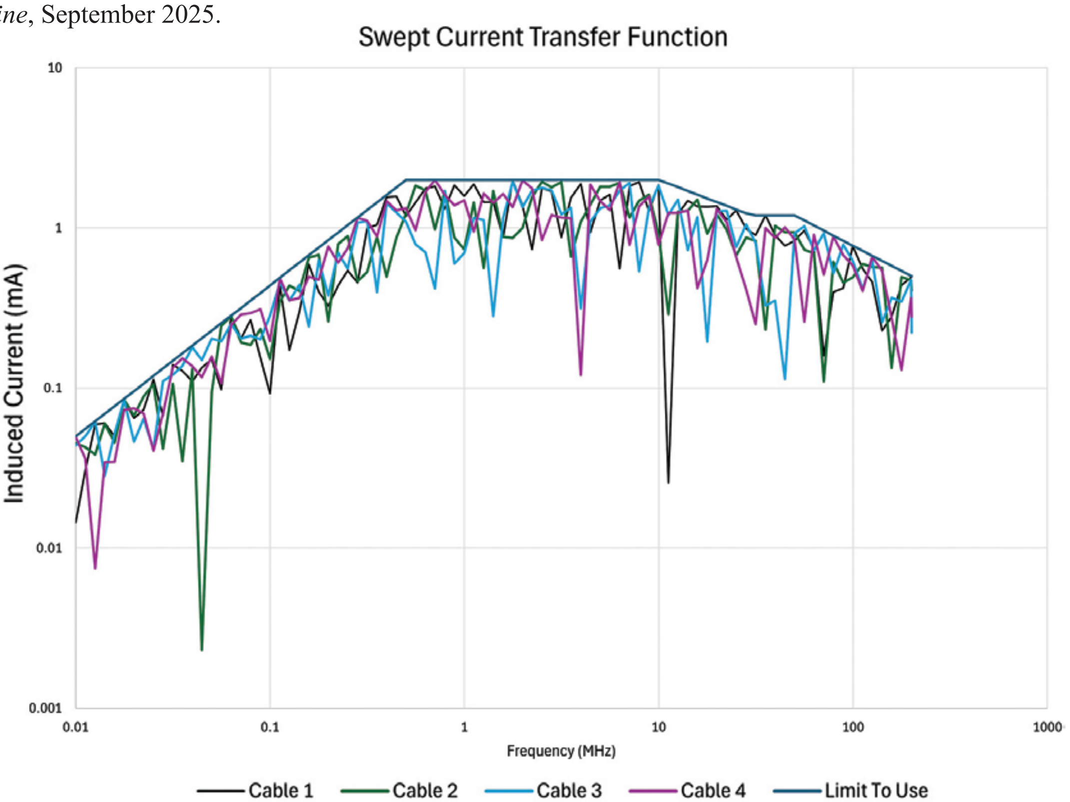

Figure 3: Induced Current During LLDD or LLSF Evaluation

ELECTRONIC WARFARE: VYING FOR CONTROL OF THE ELECTROMAGNETIC SPECTRUM

Advanced Threats Lead to Open Architecture Approaches and New Analysis of Electronic Countermeasures

Nancy Friedrich is an Aerospace Defense Solutions Expert at Keysight, specializing in EW, radar, and space and satellite modernization. Before joining Keysight, Friedrich was Executive Director and Editor-in-Chief of media brands including Electronic Design, Microwaves & RF, Design News, Power Electronics, and Machine Design. Friedrich can be reached at nancy.friedrich@keysight.com.

By Nancy K. Friedrich

Over the past decade, preeminent countries involved in major military conflicts mainly focused on asymmetrical warfare—surprise attacks by small groups armed with modern, high-tech weaponry. During that same period, however, near-peer adversaries began attaining impressive electronic warfare (EW) capabilities. As a result, a plethora of new, dynamic threats flooded the EW spectrum, pushing threat detection and analysis to keep pace.

Large military forces must now engage in ongoing development and evolution to stay ahead of their adversaries, leading to a need for a more flexible, scalable approach to threat detection, analysis, and response.

Even the smallest military can now build powerful weapons systems, given the availability and low cost of advanced electronics with high computing power. The proliferation of technology has also created a battlefield where weapons technology undergoes rapid, continuous change. Digital and programmable radio frequency equipment, such as software-defined radios, creates a more complex battlefield. In addition, radars can quickly change waveforms, making it challenging to locate, identify, and confuse hostile emitters.

These trends impact every aspect of EW, which uses the electromagnetic (EM) spectrum to sense, protect, communicate, and attack during warfare. Today, the ability to ensure spectrum-wide superiority during warfare is one of the biggest determinants of success or failure during a military operation.

ELECTRONIC WARFARE IS MODERN WARFARE

Broadly defined, EW is the use or manipulation of the EM spectrum in warfare from air, land, sea, and space. It involves the use of EM energy, directed energy, or anti-radiation weapons for uses ranging from

> While many electronic warfare systems use technology advancements such as high-performance DSP and gallium nitride amplifiers, the sheer number of possible scenarios from one threat create difficult challenges.

detection, denial, and deception to destruction and protection. EW uses radio and microwave frequencies for communications, radars, and satellites. Certain EW solutions also leverage infrared for intelligence and enemy targeting. Lasers use the spectrum to transmit data, communicate, and destroy a target.

EW includes any military action involving the use of EM and directed energy to control the electromagnetic spectrum or attack the enemy. EW comprises three main categories:

- Electronic protection involves protecting access to the EM spectrum for friendly military assets, including radio frequencies, radar frequencies, spread spectrum technology, GPS signals, and frequency coordination. Electronic protection also entails defeating electronic attacks that seek to disable the use of the EM spectrum. Examples include the use of flare rejection logic on an infrared (IR) missile, which allows a missile to function as intended despite the use of flares by an enemy to disrupt its navigation.
- EW support is broadly defined as surveillance and reconnaissance using EM energy. The data gathered can produce signal intelligence (SIGINT) to help with targeting for an electronic or physical attack. It also can produce measurement and signature intelligence.
- Electronic attack uses EM energy, direct energy, or anti-radiation weapons to confuse, disable, or destroy an enemy's electronic systems. Weapons used for electronic attack leverage lasers, electro-optical, infrared, and RF technologies.

THE PROLIFERATION OF NEW ADVANCED THREATS

Beyond their multifaceted forms and capabilities, EW threats boast high intelligence. With the increased use of adaptive programming, these systems continue to grow smarter. In response to observed effects on the battlefield, they will alter operation via radiated waveforms, techniques, or timing. Waveforms, in particular, change nearly instantaneously. Modern threats are more adaptable and reprogrammable, creating an urgent need to characterize them correctly.

The following are examples of modern warfare:

- Self-propelled decoys;
- Jamming a radar using anti-radiation missiles to foil air defenses;
- Electronic deception techniques used to confuse an enemy's intelligence, surveillance, and reconnaissance (ISR) systems; and
- Direct energy weapons with the potential to destroy people, materials, and equipment such as satellites, airborne optical sensors, and land-based forces.

Modern threats and countermeasures flood the modern EM spectral environment with thousands of emitters, including radios, wireless devices, and radar transmissions. This, in conjunction with advanced digital signal processing (DSP), creates a dramatically complex electromagnetic spectrum. DSP has led to advancements in digital dynamic range and algorithm complexity.

This environment creates complex signal activity, leading to dynamic and evolving threats for EW systems. While many EW systems use technology advancements such as high-performance DSP and gallium nitride (GaN) amplifiers, the sheer number of possible scenarios from one threat creates difficult challenges.

CHALLENGES OF ANALYZING MODERN ELECTRONIC COUNTERMEASURES

As the pace of technological change for EW outpaces developmental life cycles, threats evolve more quickly than the time it takes to build countermeasures. With the near-constant evolution of threats and

> Digital equipment can be programmed on the fly using software programs, allowing electronic warfare solutions like radars and software-defined radios to change waveforms and create unique signatures quickly.

signals in EW, militaries are investing heavily in new technologies to gain a tactical advantage and keep up with evolving threats. Many militaries find themselves engaged in a head-to-head competition, where the countermeasures catch up only to discover that the threats have moved yet another step ahead. The integration of machine learning (ML) and artificial intelligence (AI) into EW systems will help to sort through the vast array of signals and identify the correct ones on the fly.

Cognitive EW

Cognitive EW uses modern machine learning techniques to increase cognitive ability, including target recognition, intelligent decision-making, and autonomous learning. Complex and congested signal environments make it challenging to locate, identify, jam, and confuse enemy communications systems — especially if they are adaptive. For instance, adaptive radars make it challenging to isolate pulses from threatening radars, understand threats from hostile radars, and provide an adequate response.

Military technology is turning to machine learning to create cognitive EW weapons that can successfully operate in these environments. These weapons use software-defined capabilities to gain operational flexibility in congested (and contested) environments, quicker upgrades, and greater affordability.

Digital equipment can be programmed on the fly using software programs, allowing EW solutions like radars and software-defined radios to change waveforms and create unique signatures quickly. As more communications systems, radios, jammers, and IoT devices operate in the EM spectrum, spectrum awareness takes on increased importance. New EW systems look to understand the intent of each system using the spectrum, rather than relying upon assumptions about ideal scenarios regarding the environment, design/application challenge, or hardware like traditional systems. Such assumptions limit the potential for signal identification and other tasks, boosted by machine learning.

A primary challenge for electronic warfare systems is the shortened timeline for countermeasure advances compared to the long development and upgrade cycles of electronic warfare systems.

AN OPEN ARCHITECTURE TO ADEQUATELY MODEL THREATS

A primary challenge for EW systems is the shortened timeline for countermeasure advances compared to the long development and upgrade cycles of EW systems. Traditional EW solutions were designed to respond to specific, established threats that did not evolve. However, this closed-architecture approach cannot adequately respond to today's evolving EW threats due to increased component integration time, limited lifespan for parts, and a rise in technology obsolescence and refresh rates.

The procurement process also requires roughly three years for high-profile systems from order to delivery. Often, this timeline does not include further customization. Yet EW technology and threats progress at a nearly daily rate. In contrast, open architectures present a route to dynamically respond to the ever-changing threat environment.

An EW environment generation architecture that supports multiple hardware types and new technology insertion is key to keeping pace with rapidly evolving threats and reducing lead times for new systems and test capabilities. A common set of interfaces and non-proprietary file formats is also needed to develop simulator agnostic threat models that are not limited to use on only one vendor's hardware. In the U.S., for example, the Next-Generation Electronic Warfare Environment Generator (NEWEG) program allows participation from multiple vendors simultaneously via a shared interface and the use of non-proprietary formats.

Advantages of New Architectures

With open architectures, engineers can continuously evolve their EW system capabilities to meet the ongoing evaluation and testing challenges in an ever-changing EW environment. With an open architecture and scalable framework, modern simulation platforms seamlessly integrate with legacy threat databases and test methodologies while also accommodating future threat advancements across multifaceted testing programs.

Scalability is key to the performance of modern EW systems. To ensure realism and confidence in EW system performance, the industry is adopting scalable architectures that enable flexibility in the way they test from early design through mission data validation. These architectures allow test assets to be reused across multiple platforms for decades with upgrades and reliable support, maximizing efficiency and reducing cost. As EW systems become increasingly adaptive, the ability to evaluate performance against complex, evolving scenarios in a scalable, repeatable manner is essential for maintaining assurance and mitigating risk before systems are deployed in the field.

Open architectures allow testing to keep pace with the latest threat environments while enabling more precise and comprehensive EW threat simulations. With the addition of advanced analysis capabilities, engineers can also automate signal and threat model verification. The goal of such testing is to ensure that EW systems remain current and highly effective while also saving valuable time and reducing the need for additional investments in the future. Open architectures enable EW systems to remain relevant in the face of new threats by characterizing, assessing, and responding to them as needed in real-time EW scenarios.

A MORE ADAPTIVE FUTURE

Traditional military technology built on foundational systems needed additional engineering, software, and testing, and took years to complete. In today's EW environment with fast-evolving technology, this approach is no longer adequate or feasible. A system that takes two to three years to finish is obsolete before delivery.

> The warfare of the future is electronic warfare, where the EM system is the primary battlefield that every side tries to control. It's the field where computerized systems communicate, detect, attack, and protect assets.

Modern EW systems continuously evolve as new and emerging technologies transform these systems. The warfare of the future is EW, where the EM system is the primary battlefield that every side tries to control. It's the field where computerized systems communicate, detect, attack, and protect assets.

As threats evolve and change, your system must adapt. Countermeasures must also keep pace, striving to prevail over a constant stream of new threats. As the battlefield becomes increasingly crowded with devices that demand more of a limited spectrum, sorting through signals and identifying them is imperative. Future systems will move from being adaptive to using new AI and machine learning capabilities to decipher constant changes in spectrum use. Software-defined weapon technology allows for continuous upgrades without needing to invest in entirely new systems.

The new electromagnetic spectrum battlefield is increasingly challenging, and technology and weapons need to respond accordingly – even if it means breaking from the dependencies of past projects and adopting a flexible, scalable, open architecture approach.

A COMBAT SCENARIO-BASED MODEL FOR QUANTIFYING ETHICAL DECISION-MAKING IN MILITARY AI

Honyeon Kim (dxaic025.cau@gmail.com), Chulmin Yun (dxaic022.cau@gmail.com), Jinhuk Jo (herki2000@cau.ac.kr), and Joonki Paik (joonki paik@cau.ac.kr) are researchers in the Department of Artificial Intelligence at Chung-Ang University. Together, they collaborate on advancing work in artificial intelligence through their shared academic affiliation and combined expertise.

By Honyeon Kim, Chulmin Yun, Jinhuk Jo, and Joonki Paik

Editor's Note: The paper on which this article is based was originally presented at the 9th Annual International Conference on Information Technology (InCIT), held in Phuket, Thailand in November 2025. It is reprinted here with the gracious permission of the IEEE. Copyright 2025, IEEE.

In the 21st century, artificial intelligence (AI) technology has been driving a paradigm shift in defense, particularly by significantly enhancing operational capabilities in the air force domain. AI-powered combat systems support a wide range of functions such as target detection, tactical decision-making, situational awareness, and autonomous flight, thereby reducing the cognitive burden on human pilots and improving real-time responsiveness and survivability. However, the increasing autonomy of AI systems introduces complex challenges, including potential violations of international law, decision-making errors, and ambiguous attribution of ethical responsibility. This has led to a growing need to redefine the role of human fighter pilots within AI-integrated operations. To address these issues, this study proposes a quantitative ethical decision-making model that mathematically integrates national military ethics principles and international legal norms, while incorporating dynamic battlefield variables. The proposed model aims to contribute to defense policy development and combat training systems by offering a structured and operationally applicable ethical evaluation framework.

RELATED WORK

This article proposes a foundational framework for mathematically modeling ethical decision-making in AI-enabled combat systems. To support this framework, the paper examines and analyzes prior research across three key domains: 1) the development of AI technologies integrated into fighter aircraft; 2) national military ethical standards; and 3) approaches to the quantification of ethical judgment. Based on this analysis, the article emphasizes its unique and differentiated contribution to the current literature on military AI ethics.

Evolution of AI-Based Fighter Aircraft Systems

AI fighter jet technology is advancing in diverse ways depending on national strategies. The United States is pursuing unmanned–manned teaming and next-generation combat platforms through initiatives such as the Air Combat Evolution (ACE), Skyborg, and Next Generation Air Dominance (NGAD) programs. China is integrating AI pilot systems into the J-20 and enhancing the autonomous combat capabilities of AI-powered drones. Europe is focusing on AI-assisted human operations and cloud-based battlefield analysis technologies under programs like the Future Combat Air System (FCAS) and Tempest, with a strong emphasis on ethical compliance and operational safety. These developments are shifting the role of human pilots from operators to strategic decision-makers or supervisors, thereby highlighting the need for quantitative models that support ethical design and accountability frameworks.

National Standards for Military AI Ethics

As the military application of AI technologies expands, countries are establishing military AI ethics standards based on their strategic objectives and philosophical principles. The United States emphasizes responsibility grounded in practical utility, the European Union promotes legislated human-centric principles, China prioritizes state-centered strategic ethics, and South Korea remains in the early stages of institutional development.

As the military application of AI technologies expands, countries are establishing military AI ethics standards based on their strategic objectives and philosophical principles.

Trends in Mathematical Modeling of Ethical AI

Mathematical modeling approaches for evaluating ethical decision-making in AI remain limited. While theoretical models such as TOPSIS, Bayesian networks, and Markov Decision Processes (MDPs) offer frameworks for quantifying ethical judgments, they fall short in reflecting the dynamic variables of actual battlefield environments, resulting in insufficient reliability and consistency. In South Korea, the Korea Institute for Defense Analyses (KIDA) has employed the Analytic Hierarchy Process (AHP) to prioritize military AI ethical principles. However, AHP also faces limitations in accounting for the operational variability and situational dynamics of combat scenarios. Therefore, there is a growing need for research that quantitatively analyzes the sensitivity of ethical principles to combat environments and the interactions among different ethical standards.

Need for Mathematical Modeling in Military AI Ethics

Qualitative ethical judgments in the application of AI to weapon systems can lead to severe consequences, such as civilian casualties or violations of international law. Ensuring the ethical integrity of AI-enabled military systems requires the ability to quantitatively evaluate human involvement, the balance between AI autonomy and human control, and compliance with the laws of armed conflict. Given the potential conflicts among national ethical standards and the diversity of tactical environments, a mathematical model that enables consistent ethical evaluation under varying conditions is essential. Such a model must be capable of partial quantification of ethical compliance in accordance with international norms, while resolving contradictions among ethical principles.

DESIGN OF THE MATHEMATICAL MODEL

To quantitatively represent the ethical decision-making process of AI fighter pilots, this study proposes a multidimensional ethical function model (Ef) that integrates national ethical standards with the laws of armed conflict. The model is designed to enable consistent ethical judgments across diverse operational scenarios by balancing differences in national values with legal obligations.

Modeling National Ethical Standard

In designing an AI ethics model for fighter pilots, incorporating national military AI ethical principles is essential. This study derives representative ethical criteria from the United States, European Union, South Korea, and China, and formulates them into mathematical functions suitable for analysis. Each function reflects the respective country's ethical priorities and is incorporated into the overall model to ensure broad applicability and fidelity to international ethical diversity.

Country	Key Policies	Core Ethical Values
United States	AI Ethical Principles, Implementing Responsible AI	Responsibility, Reliability, Traceability, Auditability
European Union	AI Ethics Guidelines, AI Act	Human-centricity, Explainability, Legal accountability structure
South Korea	–	Human dignity, Transparency, Explainability, Safety
China	New Generation AI Ethics Guidelines	Autonomy, State Security, Social Order

Table 1: National policies on military AI ethics

United States

The ethical judgment function representing the United States incorporates the core principles outlined in the U.S. Department of Defense's AI Ethical Principles: Responsibility (*R*), Fairness (*F*), Traceability (*T*), Reliability (*Rc*), and Governability (*G*). These elements are weighted to reflect their relative importance in ethical evaluation, and the function is mathematically defined as:

$$U_i = \sum_{i=1}^{n}(w_r R_i + w_f F_i + w_t T_i + w_{re} Re_i + w_g G_i) \quad (1)$$

European Union

The European Union (EU), through its Ethics Guidelines for Trustworthy AI, identifies five core ethical principles: respect for human autonomy, prevention of harm, fairness, explicability, and transparency. In this study, a mathematical ethical decision model is defined to incorporate these principles.

$$EU_i = \sum_{i=1}^{n}(w_h H_i + w_p P_i + w_f F_i + w_x X_i + w_t T_i) \quad (2)$$

Korea

The ethical framework for defense AI in South Korea is currently under development. A study by the Korea Institute for Defense Analyses (KIDA) proposed five core ethical principles: human dignity, controllability, safety, responsibility, and explicability. In this study, a mathematical analysis model is constructed based on these principles.

$$K_i = \sum_{i=1}^{n}(w_h H_i + w_c C_i + w_s S_i + w_r R_i + w_x X_i) \quad (3)$$

China

While the ethical principles for military AI in China have not been publicly disclosed, the Chinese government outlined core national values—national security, social stability, and centralized control—in its Ethical Norms for the New Generation Artificial

Ethical evaluation in AI systems can vary significantly depending on each nation's operational doctrines, ethical philosophy, and political or strategic objectives.

Intelligence, published in 2021. This study assumes that the defense domain aligns with these national policies and accordingly defines a mathematical model for the ethical evaluation of military AI in China.

$$C_i = \sum_{i=1}^{n}(w_{ns} NS_i + w_{ss} SS_i + w_{cc} CC_i) \quad (4)$$

National Ethics Integration Model

Ethical evaluation in AI systems can vary significantly depending on each nation's operational doctrines, ethical philosophy, and political or strategic objectives. To reflect the relative influence of national ethical standards, this study introduces a set of weighting factors and defines an integrated model, National Ethics, that incorporates the core ethical principles identified by each country.

$$eN_i = \sum_{i=1}^{n}(\alpha K_i + \beta (\frac{U_i + EU_i}{2}) + \gamma C_i) \quad (5)$$

Thus, $\alpha + \beta + \gamma = 1$, $\alpha > \beta \gg \gamma)$

Mathematical Modeling of LOAC

The application of the Law of Armed Conflict (LOAC) is an essential element in the ethical decision-making process of a combat aircraft pilot. In particular, when an AI system must autonomously determine whether to employ force, it is critical to quantitatively evaluate compliance with the core principles of LOAC. To this end, the following function incorporates key LOAC principles—Military Necessity (MN), Proportionality (P), Distinction (D), Unnecessary Suffering (US), and Honor (H)—as variables for assessment.

$$LOAC_i = \sum_{i=1}^{n}(w_{mn} MN_i + w_p P_i + w_d D_i + w_{us} US_i) \quad (6)$$

Tactical Situation Modeling

Tactical situations are not static environments but are instead characterized by real-time changes within dynamic and uncertain battlefield conditions. As a result, ethical decision-making cannot rely solely on static standards; it is directly influenced by various operational variables. To reflect this, four key tactical factors are defined as variables: Situational Awareness (SA), Time Criticality (TC), Survivability (S), and Coalition Compatibility (Co). Each factor is assigned a corresponding weight $\phi_1, \phi_2, \phi_3, \phi_4$ to represent its relative importance. Based on these variables, the battlefield-context ethical evaluation function is defined as follows:

$$TS_i = \sum_{i=1}^{n}(\varphi_1 SA_i + \varphi_2 TC_i + \varphi_3 S_i + \varphi_4 Co_i) \quad (7)$$

Ethical Function Modeling

In this study, the ethical decision-making function for AI-based fighter pilots is formulated by incorporating two primary components. The first component, Ef1, represents the degree to which the AI system complies with nation-specific ethical standards. The second component, Ef2, reflects the ethical evaluation based on international laws of armed conflict. To account for the dynamic characteristics of real-world battlefield conditions, both components are modeled as functions of the tactical situation variable tactical situations.

1. *National Ethics Function Model*

The nation-specific ethics function is defined as the product of the baseline national ethical evaluation and a tactical situation adjustment coefficient. It is expressed as in:

$$Ef_1 = \sum_{i=1}^{n} TS_j \sum_{i=1}^{n} eN_i \quad (8)$$

This equation quantitatively expresses how AI ethical judgment is modulated based on both nation-specific strategic values and real-time battlefield dynamics.

2. *LOAC-Based Ethics Function Model*

The ethics function, based on the core principles of the Law of Armed Conflict, is defined as the product of those principles and a tactical situation adjustment coefficient, ensuring legal legitimacy under international law. The function is formulated as in:

$$Ef_2 = \sum_{j=1}^{n} TS_j \sum_{i=1}^{n} LOAC_i \quad (9)$$

3. *Integrated Ethical Function Model*

The integrated ethical function is constructed by combining the nation-specific ethics function Ef1 and the international law-based ethics function Ef2 using a weighting factor δ. It is formulated as in:

$$Ef = \delta \cdot Ef_1 + (1 - \delta) \cdot Ef_2 \quad (10)$$

This integrated model enhances both the consistency and flexibility of ethical judgment by accounting for a balanced consideration of strategic national values and legal principles, rather than relying on a single ethical standard.

MODEL APPLICATION AND ANALYSIS

Simulation Configuration

This simulation is based on 38 operational scenarios that a combat aircraft pilot may encounter. For both the Ef1 and Ef2 models, 100 unique combinations of parameter values were generated.

ID	Operational Situation	ID	Operational Situation
S1	Emergency air support request	**S20**	Electronic warfare decision-making
S2	Joint policing operation with allied forces	**S21**	Approaching unidentified object in restricted zone
S3	Limited airstrike in a civilian-populated area	**S22**	Determining return route after mechanical failure
S4	A-to-G mission in cooperation with autonomous UAVs	**S23**	Emergency return request from friendly aircraft
S5	Intelligence acquisition during ceasefire negotiations	**S24**	Response after detection of chemical or biological weapon
S6	Air mission to support personnel rescue	**S25**	Decision-making under communication disruption
S7	Escort mission for aircraft carrying nuclear warheads	**S26**	Assessment of civilian infrastructure threat
S8	Surprise enemy attack situation	**S27**	Recovery after AI system malfunction
S9	Night stealth infiltration operation	**S28**	Multilateral operation and alliance rules conflict
S10	Medical evacuation under enemy fire	**S29**	Response to friendly fire incident
S11	Preemptive strike on enemy command center	**S30**	Simultaneous attack and airspace conflict
S12	Response to high-altitude unmanned infiltration	**S31**	Escorting civilian aircraft under threat
S13	Maritime attack support mission	**S32**	AI weapon system shutdown decision
S14	Emergency supply transport to front line	**S33**	Target prioritization during coalition strike
S15	Protection of civilian aircraft	**S34**	Determination to protect civilian facilities
S16	Radar-evading infiltration and strike mission	**S35**	Engagement with unidentifiable hostile drones
S17	Retaliatory strike after civilian facility attack	**S36**	Ethical judgment in hostage situation
S18	Request for pilot override during AI mission	**S37**	Deployment of untested AI-based weapon system
S19	Close-range dogfight engagement	**S38**	Decision on recognition of enemy surrender gesture

Table 2: Air operation scenarios

> Analysis reveals scenarios in which the standard deviation of the ethical evaluation results was relatively high. This observation suggests that the model may exhibit instability or heightened sensitivity to fluctuations in certain conditions.

Additionally, 1,000 sets of battlefield situation variables were sampled from a normal distribution with a mean of μ=0.5\mu = 0.5μ = 0.5 and standard deviation σ=0.1. The national weighting factor (δ) was discretized into seven levels. These settings were used to conduct a sensitivity analysis of the proposed ethical evaluation functions across all scenario conditions.

Results of the Nation-Specific Ethics Function

Simulation results of the nation-specific ethics evaluation function Ef1 across all operational scenarios show the following patterns. Scenarios S14 and S22 exhibited high mean values and low standard deviations in the simulation results. This indicates that the corresponding ethical evaluations were both stable and consistent, particularly under weight combinations where Situational Awareness and Time Criticality were emphasized. These results suggest that the scenarios are ethically appropriate in terms of operational efficiency and perception-based decision-making. In contrast, scenarios S31 and S38, where the weights for Survivability and Coalition Compatibility were relatively low, produced lower ethical scores. This implies that these variables were underrepresented in the evaluation process and that ethical considerations related to battlefield stability and coalition cooperation were insufficiently incorporated.

Results of the LOAC-Based Ethical Function

The output values of the LOAC-based ethical function Ef2, assessed across all scenarios, present an analysis of the stability and sensitivity of the ethical decision structure, based on the mean and standard deviation of the ethical suitability scores derived from each scenario. Ef2 is designed to quantitatively reflect core principles of international humanitarian law, including Military Necessity, Proportionality, Distinction, Prohibition of Unnecessary Suffering, and Honor. Simulation results show that in scenarios with clearly defined ethical standards—such as S11 and S24—the evaluation outcomes remained consistent and stable. This indicates that the proposed function maintains its ethical direction and judgment criteria reliably, even under varying battlefield conditions, thereby demonstrating its potential utility as a trustworthy ethical decision-making tool in real-world combat environments.

Analysis of Unstable Scenarios

Analysis reveals scenarios in which the standard deviation of the ethical evaluation results was relatively high. This observation suggests that the model may exhibit instability or heightened sensitivity to fluctuations in certain conditions. In the case of Ef2, scenarios S29, S30, and S31 showed particularly high standard deviations, indicating inconsistency in the ethical decision-making outcomes.

This instability appears to stem from either a low weighting of tactical variables such as Situational Awareness, Time Criticality, Survivability, and Coalition Compatibility or conflicts between those variables, which hinder the model's ability to maintain coherent ethical judgments. In particular, scenario S29 presents a situation where both Time Criticality and Coalition Compatibility are simultaneously emphasized under different ethical principles. This creates a conflict in prioritization, making it difficult for the AI system to determine which standard should take precedence. As a result, Ef2 demonstrated high sensitivity, where even small variations in the input conditions led to significant changes in the ethical evaluation outcome. In the case of Ef2, scenarios S35, S37, and S19 also exhibited notable variability in ethical evaluation outcomes.

These scenarios represent situations in which priority among LOAC principles—such as Distinction, Unnecessary Suffering, and Proportionality—is ambiguous or context-dependent. As a result, the model demonstrated heightened sensitivity in the presence of legal standard conflicts. These findings suggest that while the designed model provides stable and reliable judgments in most scenarios, interpretational conflicts among ethical principles or imbalanced influence among tactical variables can lead to instability in decision outcomes. Therefore, when considering real-world deployment, it is essential to incorporate supplementary algorithms, decision deferral mechanisms, or adaptive weight adjustments to address such high-sensitivity scenarios.

Distribution of Ethical Sensitivity Across Scenarios

A total of 38 combat scenarios were classified into three distinct groups, as shown in Table 3 on page 26, based on the statistical characteristics of the ethical evaluation value (Ef) and the structural similarity of decision functions. Each group is distinguished by sensitivity indicators such as the relative weights of the α, β, and γ coefficients, as well as the mean (μ) and standard deviation (σ) of ethical outcomes.

First, the Stable Decision Group (#0) shows similar structures in both Ef1 and Ef2, with balanced α and β weights and consistently stable values for both μ and σ. These scenarios are well suited for fully automated AI-based ethical decision-making. Second, the Borderline Group (#1) exhibits relatively high average values, but with a heavier influence of β, along with greater variance.

This suggests heightened sensitivity to situational factors and the possibility of varying interpretations of ethical standards depending on context Third, the Unstable Decision Group (#2) is characterized by dominant α, suppressed β and γ values, and high standard deviations. These indicate the presence of ethical judgment conflicts and potential trade-offs between tactical variables. Such scenarios are high-risk and require mandatory human intervention in the ethical decision-making loop. This classification quantitatively demonstrates how the ethical evaluation structure of an AI combat system can vary depending on the operational scenario. It also serves as a framework for determining appropriate levels of automation, human involvement, and ethical risk for each scenario group. Moving forward, this categorization provides practical guidance for policy development, training system design, and the tailored application of ethical models according to scenario-specific characteristics.

Results of the Integrated Ethical Model

The integrated model Ethics Total, which combines the nation-specific ethics function (Ef1) and the LOAC-based ethics function (Ef2) according to a weighting parameter δ, was simulated to assess its overall performance. Compared to the individual models (Ef1 and Ef2), the integrated model demonstrated greater stability and consistency in scenario-based ethical judgments, as evaluated through quantitative metrics. The integrated model yielded lower standard deviations across most scenarios relative to the standalone models, indicating enhanced robustness of ethical outputs. In particular, when the δ value approached 0.5, the balance between national ethics and LOAC principles was optimally achieved, minimizing output variability.

However, the model still exhibited relatively high variance in certain scenarios. These cases suggest residual sensitivity due to conflicts or imbalances among tactical variables, LOAC factors, and national ethical standards. Such instability was most pronounced when multiple contextual variables

Group	Scenarios	Analysis/Policy Implications
Stable Decision Group: #0	S3, S9, S24, S27, S31, S32	- High alignment across national ethical standards enables stable judgment. - Suitable for autonomous AI decision-making. - Human-in-the-loop can be minimized.
Borderline Group : #1	S2, S5, S6, S7, S8 S12, S13, S14, S15, S16, S17, S18, S19, S20, S23, S26, S28	- Ethical judgment varies depending on the weight of specific national ethical standards (e.g., Chinese model influence). - Strategic interpretational gaps may arise. - Coordination is needed in multinational or alliance operations to prevent ethical conflicts.
Unstable Decision Group: #2	S1, S4, S10, S11 S21, S22, S25 S34, S35, S36, S37	- High sensitivity to changes in tactical situation (TS) variables. - Requires structural design for adaptive human intervention. - Needs safeguards such as judgment deferral or ethical failsafes under high uncertainty.

Table 3: Scenario-based grouping of AI ethical evaluations

conflicted simultaneously or when ambiguity in the interpretation of ethical principles was present, reducing the consistency of judgment outcomes.

CONCLUSION AND FUTURE RESEARCH DIRECTIONS

This study proposed a mathematical model that integrates nation-specific ethical standards, the Law of Armed Conflict, and tactical situation variables to quantify the ethical decision-making process of AI-based combat aircraft pilots. By applying the model across a wide range of combat scenarios, we analyzed the sensitivity and stability of AI ethical judgments under varying conditions.

The proposed framework overcomes the limitations of conventional declarative ethical standards by offering a quantitative, context-aware evaluation structure applicable to real-world operational environments, thereby laying the foundation for practical deployment and policy formulation of AI combat systems. Simulation results revealed that the ethical function responded differently depending on national values and operational contexts, and that stability and sensitivity varied across scenarios.

Particularly, scenario clustering analysis identified both stable types suitable for automated ethical judgment and high-risk types requiring human oversight. These findings underscore the necessity of context-specific, adaptive ethical system design for AI weapons systems.

For future research, several directions are proposed. First, expanding the range of tactical scenarios and incorporating multinational ethical standards will improve the accuracy and adaptability of integrated ethical models across various national and allied military forces. Second, the development of real-time decision-making algorithms, grounded in the proposed ethical function models, is essential for practical implementation in AI combat systems and training environments. Third, addressing ethical conflicts requires the design of dynamic priority adjustment mechanisms, potentially through rule-based approaches or reinforcement learning techniques. Lastly, in high-risk scenarios that necessitate human oversight, the integration of human-in-the-loop interfaces and decision-support systems will be critical to ensuring safe and effective human-AI collaboration.

This research holds both academic significance and strategic value in that it mathematically establishes ethical robustness for AI weapon systems and demonstrates its applicability in real-world military contexts. We anticipate that future efforts will extend this work toward practical implementation and global consensus-building in the domain of military AI ethics.

ACKNOWLEDGEMENT

This work was supported by the Institute of Information & Communications Technology Planning & Evaluation (IITP) grant funded by the Korea government(MND) (RS-2022-II220601, Military specialized AI Curriculum Establishment and Operation (Military AI Development and Management Program)

REFERENCES

1. J. Jae-Gyu, "A Study on Defense Artificial Intelligence Ethics," *Defense Policy Research*, vol. 39, no. 1, Korea Institute for Defense Analyses, 2023, pp. 213–240
2. H. Won-Jung, "Military Use of Artificial Intelligence from the Perspective of the Nature of War," *Korean Journal of Military Studies*, vol. 76, no. 3, Hwarangdae Institute, 2020, pp. 31–59

As AI takes the cockpit in fighter jets, who decides when to pull the trigger? This study builds a mathematical ethics model weighing national values against international law, revealing which combat scenarios AI can handle—and which demand human judgment.

3. L. Sang-Hyung, "Is Ethical Artificial Intelligence Possible? – Moral and Legal Responsibility of AI," Law and Policy Studies, vol. 16, no. 4, 2016, pp. 283–303.
4. K. Yong-Sam, "Vision and Operational Environment for the Army's Drone-Bot Combat System," Defense & Technology, no. 477, 2018, pp. 50–59.
5. K. Seung-Rae, "Legal Issues and Prospects in the Era of the 4th Industrial Revolution and AI," Law Research, vol. 19, no. 2, 2018, pp. 1–30.
6. International Committee of the Red Cross (ICRC), "The Ethical Challenges of AI in Military Decision Support Systems," ICRC Law & Policy Blog, Sep. 2024.
7. C. Batallas, "When AI Meets the Laws of War," IE Insights, Oct. 2024. [Online].
8. Z. Stanley-Lockman, "Responsible and Ethical Military AI," Center for Security and Emerging Technology (CSET), Aug. 2021. [Online]
9. M. Anneken, N. Burkart, F. Jeschke, A. Kuwertz-Wolf, A. Mueller, A. Schumann, and M. Teutsch, "Ethical Considerations for the Military Use of Artificial Intelligence in Visual Reconnaissance," Feb. 2025. [Online].
10. D. Trusilo and D. Danks, "Commercial AI, Conflict, and Moral Responsibility: A theoretical analysis and practical approach to the moral responsibilities associated with dual-use AI technology," Jan. 2024. [Online].
11. Zurek, J. Kwik, and T. van Engers, "Model of a military autonomous device following International Humanitarian Law," Ethics and Information Technology, vol. 25, art. 15, Feb. 2023
12. M. Anneken, N. Burkart, F. Jeschke, A. Kuwertz-Wolf, A. Mueller, A. Schumann, and M. Teutsch, "Ethical Considerations for the Military Use of Artificial Intelligence in Visual Reconnaissance," Feb. 2025. [Online].
13. Z. Stanley-Lockman, "Responsible and Ethical Military AI," Center for Security and Emerging Technology (CSET), Aug. 2021. [Online].
14. Kim, J. Choi, and J. Baek, "Design of an integrated function model for quantifying ethical decisions in AI fighter pilots," presented at the 2025 Annual Conference of the Institute of Electronics and Information Engineers (IEIE), Jeju, Korea, June 2025.
15. A. Hickey, "The GPT Dilemma: Foundation Models and the Shadow of Dual-Use," Jul. 2024. [Online].
16. D. Helmer *et al*., "Human-centred test and evaluation of military AI," Dec. 2024. [Online].
17. K. Cools and C. Maathuis, "Trust or Bust: Ensuring Trustworthiness in Autonomous Weapon Systems," arXiv:2410.10284, Oct. 14, 2024. [Online].
18. H. Khlaaf, S. W. Myers, and M. Whittaker, "Mind the Gap: Foundation Models and the Covert Proliferation of Military Intelligence, Surveillance, and Targeting," Oct. 18, 2024. [Online].
19. A. Nalin Tripodi, "Future Warfare and Responsibility Management in the AI-based Military Decision-making Process," J. Armed Forces Media Univ., vol. 14, no. 1, Spring 2023. [Online].
20. N. Upreti and J. Ciupa, "Towards Developing Ethical Reasoners: Integrating Probabilistic Reasoning and Decision-Making for Complex AI Systems," Feb. 28, 2025. [Online].
21. T. Izumo, "Coarse Set Theory for AI Ethics and Decision-Making: A Mathematical Framework for Granular Evaluations," Feb. 2025. [Online].
22. "Tractable Probabilistic Models for Ethical AI," in *Tractable Probabilistic Models for Ethical AI*, Springer, 2022.
23. Y. Wang, Y. Wan, and Z. Wang, "Using Experimental Game Theory to Transit Human Values to Ethical AI," Nov. 2017. [Online].

INFLUENCE OF PCB LAYOUT ON S-PARAMETER MEASUREMENTS OF HIGH-SPEED ESD PROTECTION DEVICES

How Measurement Setup Affects Accuracy in Femtofarad-Range Devices

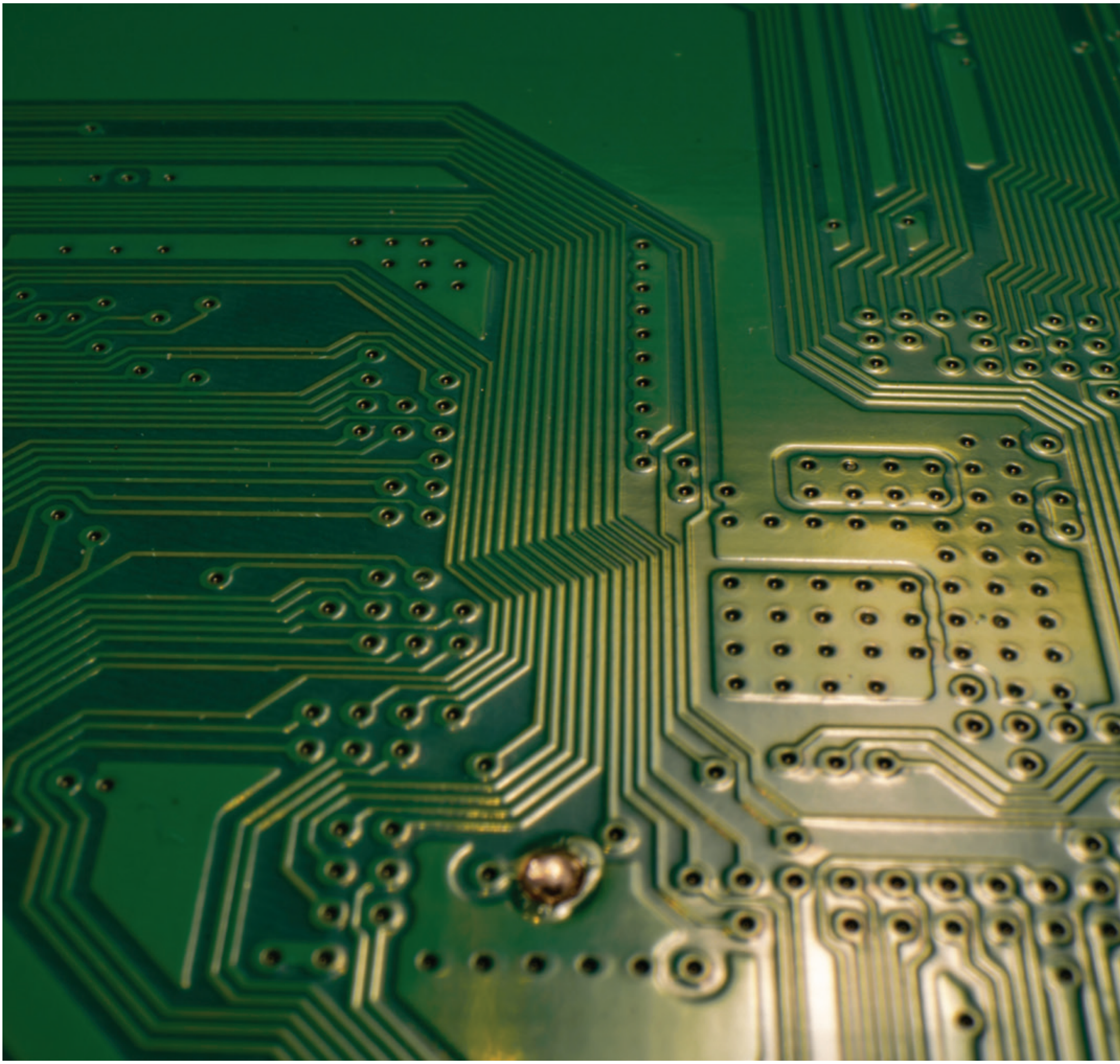

Preethi Subbaraju is a development engineer at Nexperia, with a focus on the development of ESD protection and filtering solutions. Subbaraju holds a master's degree in Microelectronics and Microsystems Technology from the Technical University of Hamburg-Harburg. She can be reached at preethi.subbaraju@nexperia.com.

By Preethi Subbaraju

ESD protection devices designed to safeguard sensitive high-speed interfaces must meet stringent signal integrity requirements. As bandwidth demand increases, these devices require increasingly lower capacitance, as shown in Figure 1. However, with the rise of high-speed applications like HDMI 2.2 and USB 4, ESD solutions should not only have smaller capacitance but must also be designed with robust signal integrity practices to ensure compliance with stringent performance standards.

Accurate and reliable measurements are vital to verify the compliance of ESD devices with interface standards, and it is critical that the measurements are not distorted by the measurement setup. In this article, we will focus on S-parameter measurements, which are widely used to characterize the high-frequency behaviour of ESD devices. As the capacitance of ESD protection devices continues to shrink into the femtofarad range, the influence of the measurement PCB and its layout on S-parameter results becomes increasingly significant.

Currently, most manufacturers of discrete ESD protection devices measure S-parameters of their devices using test PCBs compatible with 4-port Z-probes, or directly on the device using ACP probes for 2-pin devices. It is well understood that the design and quality of the measurement of a PCB can impact the signal integrity performance of the device under test (DUT). However, in many cases, these measurement PCBs are not specifically optimized for high frequency or RF performance, which can compromise the accuracy of the results.

In this article, we explore the impact of the measurement PCB on S-parameter characterization by examining ESD protection devices with two different capacitance values. We demonstrate how the PCB can affect the accuracy of the high-frequency measurements, particularly as device capacitance enters low femtofarad range. To better predict these effects, we utilize 3D electromagnetic (EM) simulations to model the device along with the measurement PCB. The simulations are validated through direct comparison to measurements, highlighting the importance of simulation-driven design and verification in ensuring accurate characterization of ESD devices.

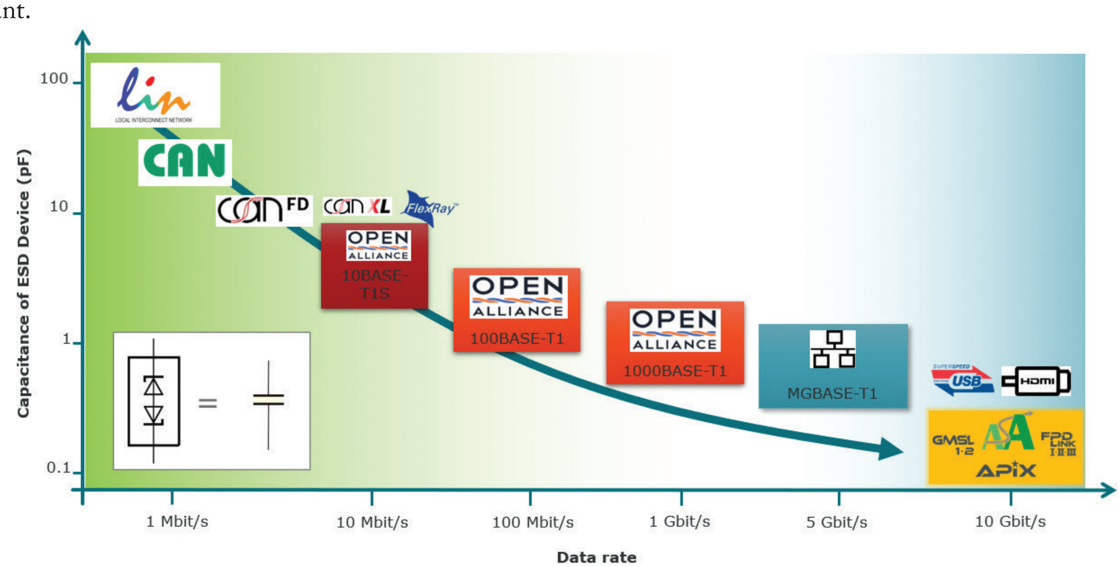

Figure 1: Capacitance trend of ESD devices for different interfaces

UNDERSTANDING INTEGRATED COMMON MODE FILTERS

Integrated common mode filters combine an ESD protection device and common mode filter in a single chip. In the event of an ESD strike, the integrated ESD protection device safely diverts the high-voltage pulse from the signal line to ground, thereby protecting sensitive downstream components. During normal data transfer, the common mode filter attenuates unwanted common mode noise that can degrade signal integrity in differential signalling systems. A simple representation of an integrated common mode filter is shown in Figure 2.

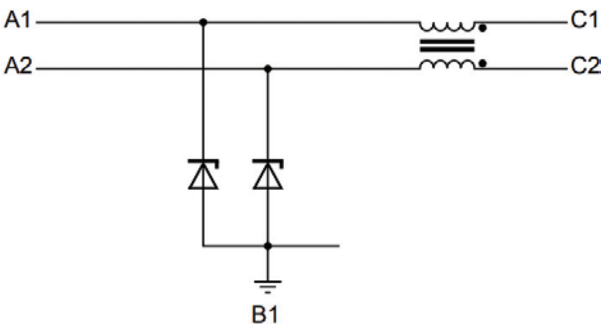

Figure 2: Schematic of integrated common mode filter with ESD protection

The advantage of using an integrated common mode filter instead of a separate common-mode filter and an ESD protection diode lies in its enhanced performance and compact design. By combining both functionalities into a single chip, these integrated solutions (referred to in this article as protection common-mode filters, or PCMFs) offer superior ESD suppression by reducing the peak voltage of an ESD pulse and provide good suppression against electromagnetic interference (EMI).

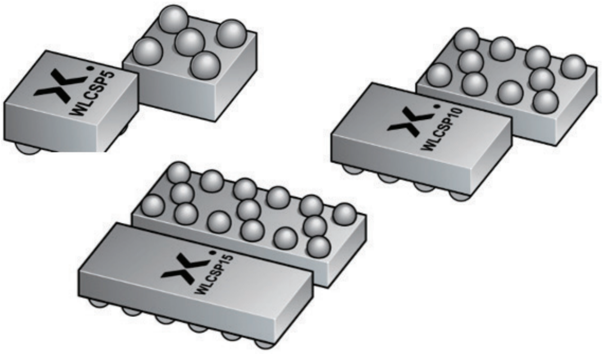

Figure 3: PCMF for 1, 2, and 3 channel protection

Furthermore, integrating both functions into a single package significantly reduces the board space and minimizes package parasitics. This reduction in package parasitics helps lower the inductance and capacitance of the overall device, thereby increasing its differential bandwidth.

PCMF devices are offered in package variants that support one, two, or three differential channels, as illustrated in Figure 3. This range of configurations provides designers with flexible protection options tailored to a wide variety of high-speed interface applications. An example of a PCB used to measure the S-parameters of the PCMFs is shown in Figure 4. This PCB is most ideal to measure the three-channel protection PCMF. But it can also be used for measuring one- and two-channel protection devices.

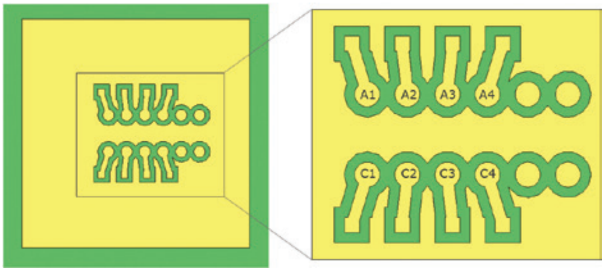

Figure 4: Top view of PCB used for measurement of S-parameters for PCMFs

The measurement PCB is a two-layer board with a top metal layer of 18um and a dielectric layer with a dielectric constant of 9.8 and a dielectric loss factor of 0.01 at 1GHz. When testing a one-channel PCMF device, it can be mounted in either of two positions on the PCB: A1–A2/C1–C2 (referred to as Position 1) or A2–A3/C2–C3 (referred to as Position 2), as illustrated in Figure 5.

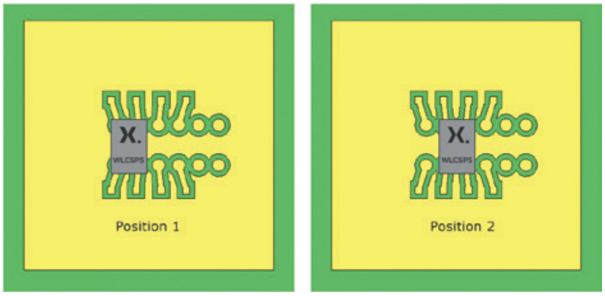

Figure 5: Placement of PCMF on measurement PCB showing position 1 and position 2

When the PCMF is placed in position 1, the differential traces used for measurement are asymmetric, with unequal lengths and inconsistent spacing between them. This asymmetry may cause signal integrity issues that are not immediately apparent through basic analysis.

When we use a standard impedance trace calculator to estimate the impedance of the PCB traces, it may show that the characteristic impedance of the PCB lines is around 50 Ohms, as they typically assume uniform trace lengths and consistent spacing to the ground. But they do not count for the impedance discontinuity when the spacing to the ground plane is varied, which can lead to signal reflections and increased insertion loss, effects that are difficult to estimate from traditional calculations or simple equivalent circuit simulations.

To address this, 3D electromagnetic (EM) simulations offer a powerful and efficient way to model the complete PCB structure, including all geometric and material complexities.

USING 3D EM SIMULATIONS TO ESTIMATE DEVICE S-PARAMETERS

3D EM models of the PCMFs are created by incorporating the metal structures and dielectric layers of the device, along with the package details accurately modelled with material specifications required for EM simulations. The active region of the ESD diode within the PCMF is modelled as a discrete capacitor. The ESD diode junction capacitance is initially roughly estimated based on device design, then fine-tuned by comparing simulation results to measured data. Once the discrete capacitance value of the ESD diode model is validated, the same ESD diode model can be used for predicting the bandwidth performance of the device across different package configurations.

For these simulations, we utilize a powerful tool for high-frequency 3D EM modelling.[1] To ensure accurate correlation between simulation and measurement, the PCB used for measurement is also included in the simulation environment. This allows for a realistic representation of the measurement setup, including all parasitic effects introduced by the board.

The differential insertion loss of a PCMF device (referred to as PCMFa) is simulated in position 1 and position 2 of the measurement PCB, which are shown in Figure 5. The simulation results are compared to measurements as shown in Figure 6. The correlation between simulation and measurement is quite good up to 30GHz, demonstrating the accuracy and reliability of the modelling approach.

IMPACT OF MEASUREMENT PCB ON S-PARAMETER CHARACTERIZATION

The differential S-parameters of a state-of-the-art PCMF, PCMFa used for HDMI and USB standards are measured using the measurement PCB in both position 1 and position 2. The resulting differential insertion loss Sdd21 is presented in Figure 7. From the graph, we can clearly see that the differential insertion loss and the differential bandwidth of the device are highly influenced by the measurement position on the PCB. We can see that the PCB influences the device at high frequencies above 10GHz. When the device is measured in position 2, there is a gain of nearly 7GHz in differential cutoff frequency.

This strong dependence on PCB layout is primarily due to the extremely low capacitance of the ESD diode (on the order of femtofarads) and the small inductance values of the common-mode filter, typically in the nanohenry range. In such cases, the impedance discontinuity introduced in the PCB due to asymmetric traces and varying spacing to ground can have a pronounced impact on the measured performance.

When we measure a different PCMF, PCMFb, which has nearly two times higher inductances of the common mode filters and capacitance of the ESD diodes, the influence of the PCB becomes less significant. As shown in Figure 8, the differential insertion loss for PCMFb exhibits much smaller variation between the

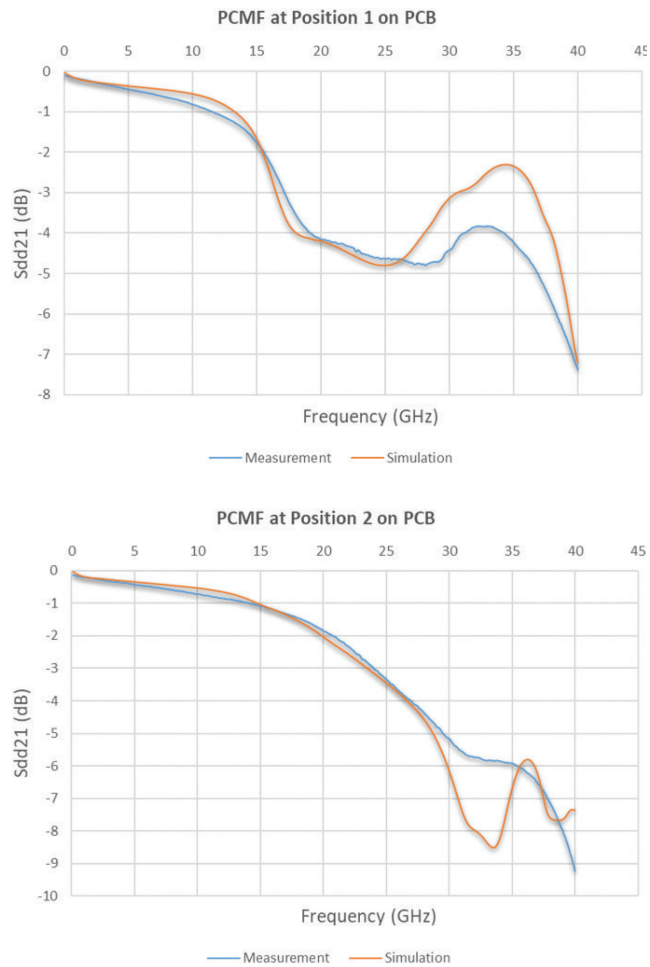

Figure 6: Validation of simulation of PCMFa in position 1 and position 2 on the PCB by comparing to the measurement

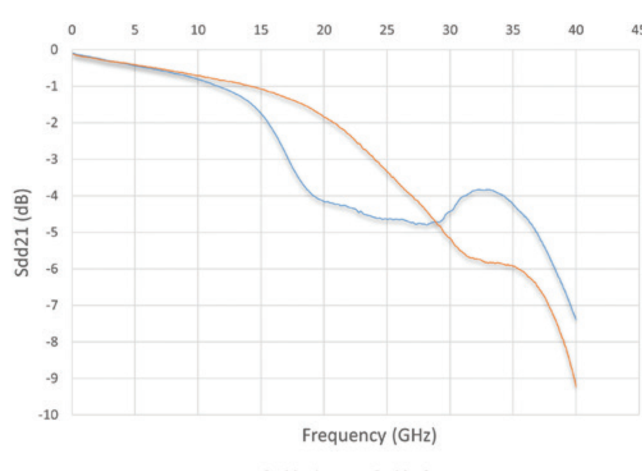

Figure 7: Differential insertion loss measurement of PCMFa on position 1 and position 2 on PCB

two measurement positions. This indicates that the device's intrinsic electrical characteristics dominate its performance, making it less sensitive to the measurement PCB.

CONCLUSION

As high-speed digital interfaces continue to evolve, the demand for ESD protection devices that offer both ultra-low capacitance and excellent signal integrity performance has never been greater. This article has highlighted the critical role that accurate S-parameter measurements play in verifying the compliance of these devices with modern interface standards such as HDMI 2.2 and USB4. However, as demonstrated, the accuracy of these measurements is highly dependent on the design and quality of the measurement setup, particularly the PCB used during testing.

Through measurements and 3D EM simulations, we have shown that variations in PCB layout, such as trace asymmetry and inconsistent spacing to the ground plane, can significantly affect the performance of ESD protection devices, especially those with capacitance in the femtofarad range. The use of advanced simulation tools enables designers to model these effects with more accuracy, allowing for better prediction and optimization of device behavior in real-world conditions.

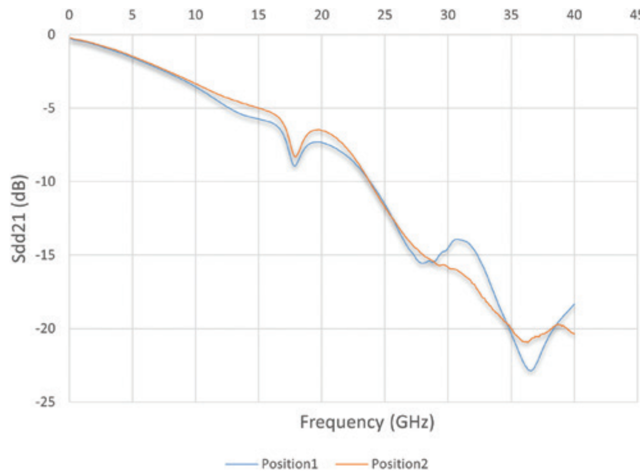

Figure 8: Differential insertion loss measurement of PCMFb on position 1 and position 2 on PCB

Ultimately, this article underscores the importance of co-designing ESD protection devices and their measurement environments. By combining accurate modelling, careful PCB design, and robust measurement practices, engineers can ensure that ESD protection solutions meet the stringent demands of today's high-speed digital systems.

ENDNOTES

1. CST Studio Suite by Dassault Systèmes, 05 June 2025.

IMPACT OF PCB VIA AND TRACE GEOMETRY ON THE EFFECTIVENESS OF DECOUPLING CAPACITORS

Part 1: Board Topologies and the PCB Circuitry

By Bogdan Adamczyk, Allyson Telck, and Scott Mee

This is the first of several columns investigating the effectiveness of decoupling capacitors while varying the topology of vias, trace length between the decoupling capacitor and the integrated circuit (IC) power/ground pins, and distance from the internal power and ground plane pair. Specifically, the impact of the PCB geometry will be evaluated by performing RF Emission testing on six PCB variants, according to the CISPR 25 standard. Part 1 of this study defines the board topologies and the PCB circuitry. The following parts will show the RF Emissions results.

Dr. Bogdan Adamczyk is professor and director of the EMC Center at Grand Valley State University (http://www.gvsu.edu/emccenter) where he performs EMC educational research and regularly teaches EM/EMC courses and EMC certificate courses for industry. He is an iNARTE-certified EMC Master Design Engineer. He is the author of two textbooks, "Foundations of Electromagnetic Compatibility with Practical Applications" (Wiley, 2017) and "Principles of Electromagnetic Compatibility: Laboratory Exercises and Lectures" (Wiley, 2024). He has been writing "EMC Concepts Explained" monthly since January 2017. He can be reached at adamczyb@gvsu.edu.

Allyson Telck is participating in a combined degree program to earn a Bachelor of Science in Electrical Engineering and a Master of Science in Biomedical Engineering at Grand Valley State University. She recently completed her final rotation as an Electromagnetic Compatibility Engineering co-op student at E3 Compliance, which specializes in EMC and high-speed design, pre-compliance testing, and diagnostics. She can be reached at allyson.telck@e3compliance.com.

Scott Mee is a co-founder and owner at E3 Compliance, which specializes in EMC & SIPI design, simulation, pre-compliance testing, and diagnostics. He has published and presented numerous articles and papers on EMC. He is an iNARTE certified EMC Engineer and Master EMC Design Engineer. Mee participates in the industrial collaboration with GVSU at the EMC Center. He can be reached at scott.mee@e3compliance.com.

SCHEMATIC OF THE PCB CIRCUITRY

Figure 1 shows the circuit schematic. The PIC10F200 microcontroller [1] was programmed to blink three LEDs using PWM [2]. To keep the current of each I/O pin below the allowable maximum of

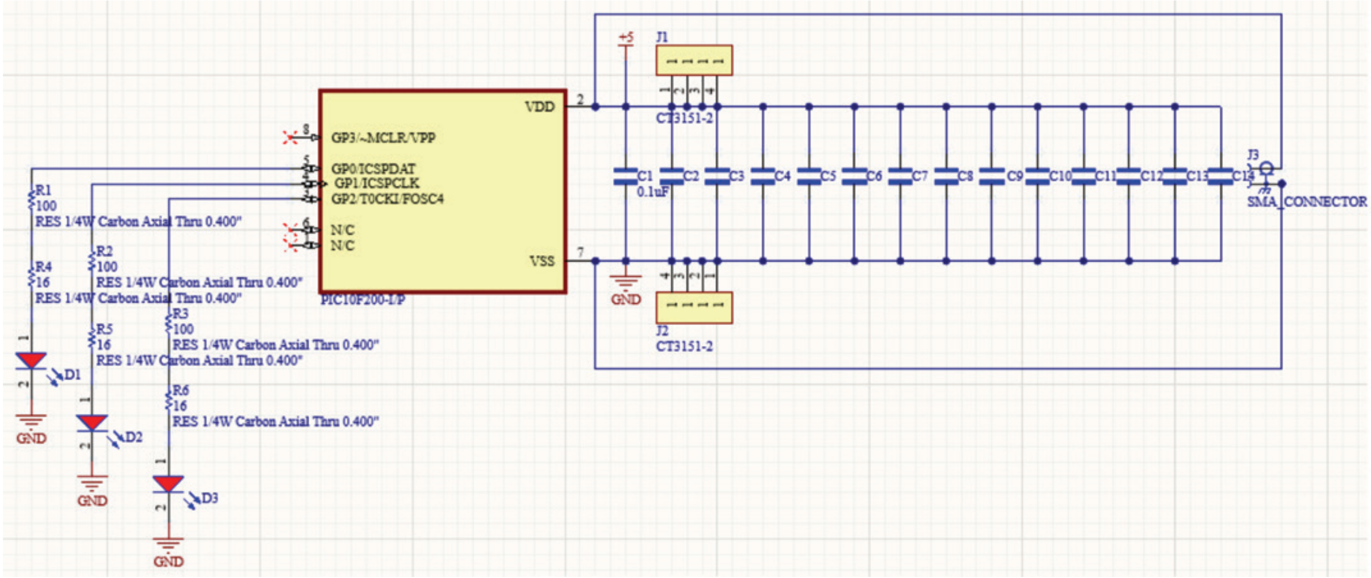

Figure 1: Circuit schematic

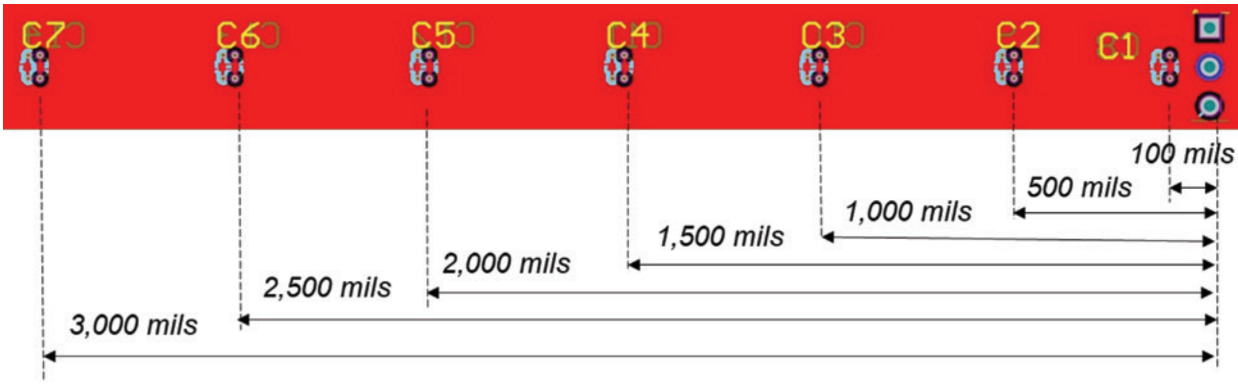

Figure 2: Block of the capacitor pads

25 mA rating, each LED was wired in series with a resistance of 116 Ω. Fourteen 0402 capacitor pads were grouped in two blocks of seven, as shown in Figure 2.

One block (C1 – C7) of pads was on the top layer, while the other (C8 – C14) was on the bottom layer. The first pad in each block was 0.1 inch away from the PWR and GND pins of the IC, while the remaining six pads were placed at 0.5-inch distance increments. Only one pad at a time was populated with a 0.1 µF X7R capacitor, [3].

VIA AND TRACE TOPOLOGIES

Six PCBs were designed incorporating the capacitor placements explained above, but each variant had a different via topology, as shown in Figure 3.

Board A had four vias connected to the capacitor. Two vias led to the board's internal power plane and were placed on either side of the capacitor's power pin, approximately 0.03 inches away from the center of the pin pad. The other two led to the board's internal ground plane and were placed on either side of the capacitor's ground pin at the same distance. 0.03 inches separated each power and ground via pair. Straight traces connected the vias to the capacitor.

Board B was similar to Board A but had only two vias connected to the capacitor instead of four. The via leading to the internal power plane was placed 0.03 inches above the capacitor's power pin, while the via leading to the internal ground plane was placed 0.03 inches above the capacitor's ground pin. Again, there was 0.03 inches of separation between the power via and the ground via.

Board C had two vias connected to the capacitor, where one was approximately 0.026 inches to the

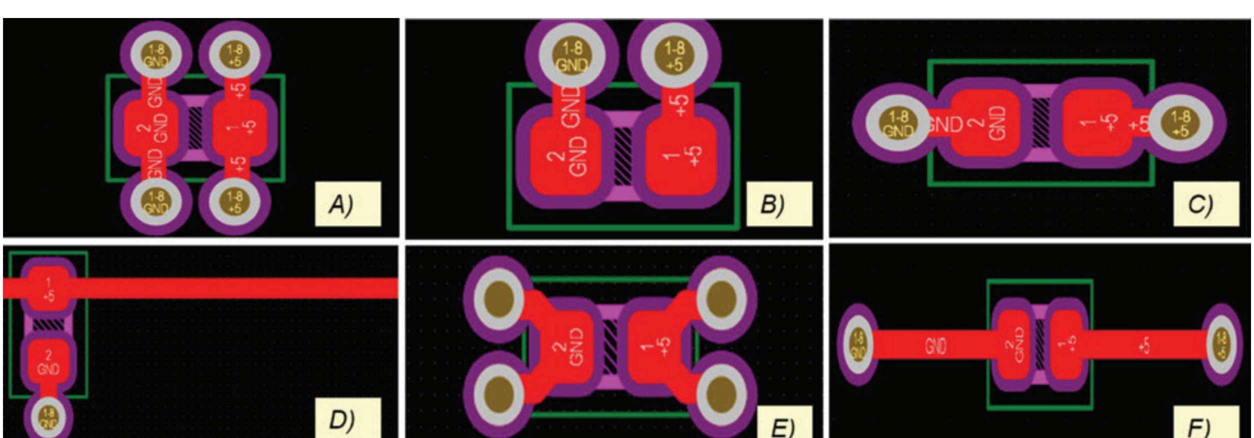

Figure 3: Different via topologies for each PCB

Small changes in a PCB layout can make or break decoupling capacitor performance. This study compares six different via topologies—from single-via designs to four-via configurations—to see which approaches reduce RF emissions and which fall short.

left of the capacitor's ground pin, and the other was 0.025 inches to the right of the capacitor's power pin. 0.085 inches separated the vias from each other.

Board D used only one via, which connected to the board's internal ground plane and was placed approximately 0.026 inches away from the center of the capacitor's ground pin. A long trace ran from the capacitor's power pin to the PIC10F200's power pin.

Board E had four vias connected to the capacitor. Each via was placed at a vertical distance of approximately 0.015 inches and a horizontal distance of approximately 0.026 inches from the center of the respective capacitor pin. This left 0.086 inches of distance between each power and ground via pair. The traces connecting the vias to the capacitor pin pads were also curved.

Board F was similar to Board C but had a longer trace between each via and the capacitor. Each via was approximately 0.1 inches from the center of its respective capacitor pin pad, making the distance between the vias 0.234 inches.

PCB TOPOLOGY

In our study, we used a six-layer PCB [4] with the topology shown in Figure 4.

1 oz Cu was used for the outer layers, while ½ oz Cu was used for the inner layers. Closely-spaced power and ground plane pair is closer to the top layer than the bottom layer. This impacts the current loop area and thus the loop inductance during switching. Ground planes had no pullback distance from the board edges, while the power plane was pulled back a distance of 20H, with H being the thickness of the core.

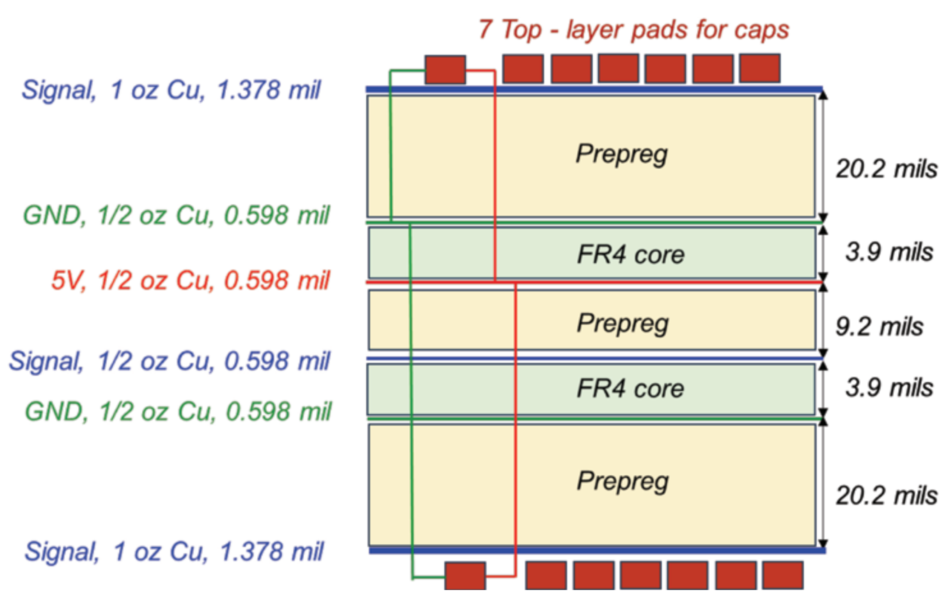

Figure 4: Topology of the 6-layer PCB

FUTURE WORK

The next article in the series will discuss the measurement setup and the test results of the conducted emissions according to CISPR 25 regulations.

REFERENCES

1. https://ww1.microchip.com/downloads/en/DeviceDoc/40001239F.pdf
2. https://www.we-online.com/components/products/datasheet/151051RS11000.pdf
3. https://www.digikey.com/en/products/detail/yageo/CC0402KRX7R9BB104/5883371
4. https://jlcpcb.com

SMALL FORM FACTOR CDM TESTING

Part 2: Air Discharge Options

By Kathleen Muhonen for EOS/ESD Association, Inc.

Kathleen Muhonen is a Principal Development Engineer at Qorvo, specializing in ESD protection and instrumentation. She serves on ESDA device testing standards committees and holds a Ph.D. in EE from Penn State, with prior roles at HP and Lockheed Martin.

Founded in 1982, EOS/ESD Association, Inc. is a not for profit, professional organization, dedicated to education and furthering the technology Electrostatic Discharge (ESD) control and prevention. EOS/ESD Association, Inc. sponsors educational programs, develops ESD control and measurement standards, holds international technical symposiums, workshops, tutorials, and foster the exchange of technical information among its members and others.

This column is the second in a three-part series on testing small form factor products for CDM. Part 1 highlighted the issues of CDM testing with the current field-induced CDM (FICDM) testers. The main problems are the pogo pin size vs package or ball bump size and that small form factor products may have very low withstand voltages, where the FICDM testers are known to be unreliable. In Part 2, the first set of possible solutions is presented. These solutions are air discharge techniques just like FICDM. Part 3 will focus on contact-first methods to address these same issues.

AIR DISCHARGE OPTIONS FOR BARE DIE AND INTERFACE DIE TESTING

CDM Tester with Small Probe to Contact Bare Die Bumps or Pads

A wafer CDM tester is shown in Figure 1. This tester was built by modifying a standard FICDM tester [1]. The basic configuration matches the hardware platform prescribed by ANSI/ESDA/JEDEC JS-002 [2]. To make contact with the small pads of bare die or wafer, the tester has a 7-µm radius needle connected to a ground plane with 1-ohm resistance. One end of the 1-ohm resistor is connected to the inner conductor of the coaxial cable, while the other end is connected to the ground plane and to the shield conductor of the coaxial cable. The coaxial cable is connected to an oscilloscope. There is a charge plate that can hold a 300-mm wafer.

A 1.8V power terminal that had experienced frequent failures at the assembly house. This modified tester was used to test the product in three different form factors: first on wafer of 300 mm at full thickness, second bare die which was 8 x 8 mm and a thickness of 400 µm,

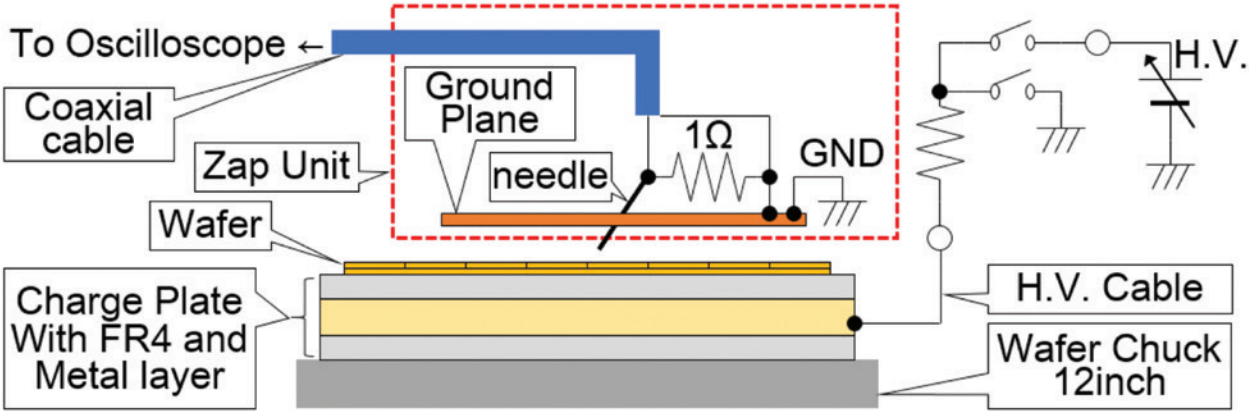

Figure 1: Wafer CDM tester – Block diagram

and finally in a BGA package at 30 x 30 mm in size. The results are shown in Table 1.

For the 1.8V power terminal, the destruction voltage for the bare die and wafer tests was, respectively, 1500V and 1250V, which easily met the electrostatic control standard of 200V. This shows that electrostatic controls at the assembly house were inadequate and consistent with the level of failures seen. This method does provide a solution to gather on-wafer CDM data, but it does not address the lower voltage stability issues that FICDM testers are known to have. Odds are this still needs to be addressed.

Contact First CDM (CF-CDM)

The contact first with air discharge approach to CDM was developed to address two aspects of field-induced air discharge CDM testing, one of which is especially important for fine pitch packaged devices, and when stressing bare die or at the wafer level.

- A sharp tip degrades the arc's properties in air discharge. This method removes that degradation because the discharge is in the chamber, not at the sharp-tip pogo pin.
- Air discharge quality and repeatability depend on air quality, such as humidity.

An entirely new ground plane and test head were developed and are shown in Figure 2. The ground plane includes a contact pin, which is physically but not electrically connected to the ground plane. The ground plane is lowered in operation until the contact pin touches the DUT. Since the contact pin is floating and has low capacitance, it does not ground the DUT. Next, the rest of the test head continues its downward motion until an air discharge occurs between the pogo pin and the top of the contact pin, very similar to the discharge of a standard FICDM. The discharge pogo pin is connected to the 1-ohm resistor and current measurement electronics. The top of the contact pin and the discharge pogo pin are enclosed in a small chamber flooded with dry nitrogen. This method provides a spark geometry independent of contact geometry. The discharge also occurs in a stable, dry nitrogen environment, eliminating the issue of humidity [3].

	Bare die	Package	Wafer
1.8V power terminal	1500V	1300V	1250V

Table 1: Product test results

Measurement results with the contact first air discharge CDM method were found to meet the requirements of ANSI/ESDA/JEDEC JS002 regarding waveform parameters such as peak height, rise time, peak width, and undershoot, but unfortunately, only marginally better regarding variability from arc to arc. The real strength of the new system has turned out to be its ability to reliably test packages with very fine pitch connections. The method allows using a sharp contact pin to touch the DUT before any discharge.

SUMMARY

The standardized FICDM tester with a pogo pin is unsuitable for bare-die or wafer-level (including 2.5D/3D microbump D2D interfaces) CDM testing. The two air discharge options in the literature today approach the problem differently. One system uses an FICDM tester and modifies it so that it can handle wafers to be charged. It also has a modified pogo pin to contact the pads/bumps on the part. Limited data is available that proves its usefulness as an option for small form factor parts. The second system can contact

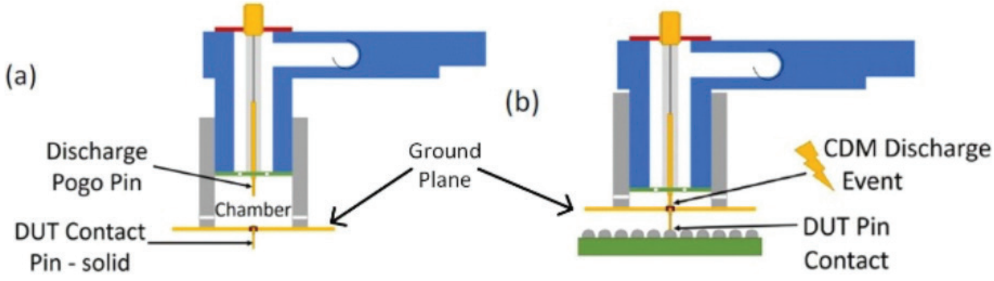

Figure 2: Contact first CDM test head, (a) with head separated from DUT and (b) shown in the stress position

the part with a secondary small pogo pin. Air discharge takes place in a chamber above the small pogo pin as the primary pogo pin will drop after the smaller pogo pin has made contact. In Part 3, another set of systems will be presented that do not have an air discharge. The associated pros and cons will also be discussed.

ACKNOWLEDGEMENTS

This three-part publication is part of a summary of a technical report published by the ESD Association. The authors of that technical report would like to be acknowledged here: Robert Ashton (retired), David Epps (AMD), Jared Floyd (ESDEMC), Wei Huang (ESDEMC), David Klien (pSemi), Tom Meuse (Thermo Fisher), Kathleen Muhonen (Qorvo), Friedrich sur Nieden (Infineon), Paul Phillips (Phasix), Michael Reardon (ESDEMC), Masnori Sawada (Hanwa), Jasmine Shen (ESDEMC), Marko Simicic (IMEC), Heinrich Wolf (Fraunhofer)

REFERENCES

1. M. Sawada et al., "Study of FI-CDM Discharge Waveforms," EOS/ESD Symposium 2010.
2. ANSI/ESDA/JEDEC JS-002, *Charged Device Model (CDM) - Device Level*, EOS/ESD Association.
3. Grund et al., "A New CDM Discharge Head for Increased Repeatability and Testing Small Pitch Packages", EOS/ESD Symposium 2018.
4. Kathleen Muhonen, "Small Form Factor CDM Testing, Part 1: Problems with FICDM Testing for Small Form Factor and Interface Die," *In Compliance Magazine*, January 2026.

PRODUCT Showcase

Technical Library

Whitepaper

Mastering High Voltage: The Importance of Accurate Test Equipment

This whitepaper underscores that precise calibration of high-voltage test gear—especially when measuring 1 kV–150 kV systems—is essential for safety, reliability, and regulatory compliance. It details measurement techniques (voltage dividers, step-down transformers, etc.), the impact of environmental and connection factors on accuracy, and why traceable calibration (e.g., to NIST/A2LA) is a must to ensure consistent, reliable results.

offered by VITREK

Guide

How to Become A Great Compliance Engineering Professional

The journey to becoming an excellent compliance engineering professional is an ongoing process of continuous learning, practical skill development, and unwavering commitment to ensuring product safety, regulatory compliance, and maintaining the highest standards of professional integrity.

Primer

A Dash of Maxwell's: A Maxwell's Equations Primer

Through mathematical precision, Glen Dash offers a comprehensive exploration of Maxwell's Equations, revealing the intricate mechanisms by which electric and magnetic fields interact to explain electromagnetic radiation and fundamentally shape our technological understanding of modern electronics and communications.

http://incompliancemag.com/technical-library

Advertiser Index


OPHIR RF
High Power RF Amplifiers
CALL US!
(310) 306-5556
MADE IN USA
Since 1992
www.OphirRF.com